From the Division of Clinical Geriatrics
Department of Neurobiology, Care Sciences and Society
Karolinska Institutet, Stockholm, Sweden

MAGNETIC RESONANCE IMAGING AND SPECTROSCOPY IN AT-RISK POPULATIONS AND PRECLINICAL ALZHEIMER'S DISEASE.

Olga Voevodskaya

Karolinska Institutet

Stockholm 2018

Cover illustration by Olga Voevodskaya
All previously published papers were reproduced with permission from the publisher.
Published by Karolinska Institutet.
Printed by E-print AB 2018

ISBN 978-91-7831-065-4

Magnetic resonance imaging and spectroscopy in at-risk populations and preclinical Alzheimer's disease

THESIS FOR DOCTORAL DEGREE (Ph.D.)

By

Olga Voevodskaya

Principal Supervisor:
Associate professor Eric Westman
Karolinska Institutet
Department of Neurobiology,
Care Sciences and Society
Division of Clinical Geriatrics

Co-supervisors:
Professor Lars-Olof Wahlund
Karolinska Institutet
Department of Neurobiology,
Care Sciences and Society
Division of Clinical Geriatrics

Professor Oskar Hansson
Lund University
Department of Clinical Sciences
Clinical Memory Research Unit

Dr. Andrew Simmons
King's College London
Department of Neuroimaging

Opponent:
Associate professor Paul Unschuld
University of Zurich
University Hospital for
Psychogeriatric Medicine

Examination Board:
Associate professor Stina Syvänen
Uppsala University
Department of Public Health and Caring Sciences

Professor Maria Engström
Linköping University
Department of Medical and Health Sciences

Associate professor Weili Xu
Karolinska Institutet
Department of Neurobiology,
Care Sciences and Society
Aging Research Center

ABSTRACT

Alzheimer's disease (AD) is the most common form of dementia. One of the earliest and most distinct features of AD is memory loss, followed by difficulties in learning and a decline in cognitive abilities. People afflicted with AD usually develop symptoms in their late seventies, but we know today that the very first signs of pathology can be detected decades before symptom onset. A considerable part of AD research today is focused on the detailed characterization of this asymptomatic "silent" phase of AD.

The main pathological hallmarks of AD are amyloid plaques – abnormal extracellular deposits of the amyloid-β (Aβ) protein and intracellular neurofibrillary tangles (NFTs) – aggregates of the phosphorylated tau protein. AD is also characterized by progressive neurodegeneration – a deterioration of the structure and function of neurons, which leads to loss of brain tissue. Atrophy first takes place the medial temporal lobe (the entorhinal cortex and the hippocampus) and subsequently propagates to other areas of the brain. Magnetic resonance imaging (MRI) is a powerful method used to assess the extent of atrophy of the whole brain or specific structures. Another useful tool for studying AD pathology is magnetic resonance spectroscopy (MRS). This method allows quantification of certain brain metabolites *in vivo*. The most relevant MRS metabolites in the context of AD are myo-inositol – an organic osmolyte and N-acetyl-aspartate – a marker of neuronal integrity.

The overall aim of this thesis is to further characterize structural and metabolic changes associated with incipient AD pathology.

Study I assesses a common methodological issue of volumetric MRI studies related to inter-individual differences in intracranial volume (ICV). In a study setting where regional brain volumes are analyzed, it is often of interest to compare groups, e.g. control vs patient, in order to quantify atrophy due to pathology. This type of group comparison is confounded by the fact that people with larger ICV usually have larger brain structures, making it difficult to isolate disease-related atrophy. This work examines multiple procedures that can be used to compensate for ICV in volumetric studies, highlighting that the choice of ICV normalization approach may have profound effects on the interpretation of study results.

Study II examines brain morphology from a network perspective. Here, the brain is represented as a graph – a set of nodes interconnected by edges – where the nodes are based on anatomical regions and the edges are measures of the "connection" (i.e. structural co-variance) between these regions. We examine global and local network properties in cognitively healthy elderly with evidence of amyloid pathology. **Study II** reveals that the changes in cerebral network topology in asymptomatic individuals at risk for AD occur before to any detectable cortical thinning.

Studies III and IV explored whether brain metabolites measured with MRS may be useful biomarkers of ongoing amyloid-related pathological processes. Previous MRS studies have found that in a typical AD spectrum, mI is elevated and NAA is decreased. However, relatively

little is known about the time course of these changes as well as the interplay between MRS and established biomarkers/risk-factors for the disease. In **Study III**, MRS spectra of non-demented individuals at varying degrees of risk for AD was examined in conjunction with information about Aβ, tau and APOE ε4 carriership – the main genetic risk factor for AD. Our findings highlight the very early involvement of brain mI in AD. We show that this metabolite is changed already at presymptomatic disease stages, and that elevated mI is linked to a higher Aβ plaque load. **Study IV** is an extensive follow-up of Study III, and the first longitudinal MRS study, taking into account individual amyloid status. We demonstrate that during a four-year follow-up, non-demented individuals with pathological baseline Aβ accumulate mI at a higher rate, suggesting that mI may have the ability not only to detect but also to track ongoing Aβ pathology. Ultimately, we hope that non-invasive cost-efficient MRS markers may be useful for early patient screening and evaluation of disease-modifying strategies.

SAMMANFATTNING PÅ SVENSKA

Alzheimers sjukdom är den vanligaste formen av demenssjukdom. Personer som lider av Alzheimer drabbas av en försämrad minnesfunktion, inlärningssvårigheter och nedsatt kognitiv förmåga.

Forskning har visat att de tidigaste patologiska processerna kopplade till Alzheimers sjukdom inträffar 10-20 år innan de första symptomen uppträder. De inledande förändringarna i hjärnan uppstår när proteinet β-amyloid ansamlas i hjärnbarken i så kallade amyloida plack. Det andra kännetecknet på Alzheimer är spridningen av ansamlingar av det patologiska proteinet tau. Alzheimer är en neurodegenerativ sjukdom där nervceller förtvinas och så småningom dör, vilket leder till att vissa områden i hjärnan minskar i volym. De områden som först drabbas av nervsönderfall är de mediala temporalloberna (entorhinalcortex och hippocampus) och med tiden sprider sig atrofin genom hela hjärnan. Även subtila förändringar i hjärnvolym går idag att mäta tack vare avancerade bildgivande metoder, framförallt magnetresonanstomografi (MRT). Förutom att studera atrofi går det även att undersöka förändringar av vissa kemiska ämnen i hjärnan. Metoden som möjliggör detta heter magnetresonansspektroskopi (MRS) och kan tillämpas i samband med en rutinundersökning med MR. Metaboliternas koncentrationer avspeglar det allmänna hälsotillståndet hos hjärncellerna, ämnesomsättning i hjärnan och eventuellt även amyloid-patologi in vivo.

Idag finns inga botemedel mot Alzheimer, däremot finns symptomlindrande läkemedel som oftast är effektiva i början av sjukdomsförloppet. Att kunna upptäcka sjukdomen i ett tidigt skede är en förutsättning för att så småningom lyckas utveckla en framgångsrik behandling. Därför går en stor del av Alzheimerforskning idag ut på att hitta och validera nya sjukdomsmarkörer samt avbilda de allra tidigaste patologiska förändringar i hjärnan.

Avhandlingens syfte är att bidra till kartläggningen av strukturella och metaboliska förändringar i hjärnan vid begynnande Alzheimer. Därför har vi företrädesvis arbetat med data från individer med tidiga tecken på kognitiv svikt samt friska personer i riskzonen för Alzheimer, snarare än patienter med fastställd demensdiagnos. I avhandlingen ingår fyra delarbeten, de två första är inriktade på hjärnans anatomi/morfologi och de två sista undersöker hjärnans metabolism.

Studie I behandlar en viktig metodologisk aspekt av volymmätningar av olika hjärnstrukturer. I studier där regionala hjärnvolymer analyseras är det ofta intressant att jämföra dessa strukturer mellan grupper (t.ex. friska och sjuka) för att kvantifiera volymminskningen orsakad av sjukdomen. Dessa gruppjämförelser försvåras av att människor med större huvuden oftast även har större hjärnstrukturer. För att komma fram till ett pålitligt resultat måste en kompensation för den intrakraniella volymen (ICV, från eng. intracranial volume) tillämpas. Studien redogör för de olika normaliseringsmetoderna och belyser för- och nackdelar med samtliga. Arbetet belyser att det sätt man använder för att ta hänsyn till ICV kan vara direkt avgörande för tolkningen av resultat i volymetriska studier.

I **Studie II** använder vi oss av det matematiska konceptet grafteori för att studera strukturella förändringar i hjärnans nätverk. Grafteori är en kraftfull metod som bland annat undersöker förmågan hos nätverken att snabbt integrera information från avlägsna områden i hjärnan, samt stå emot anfall. En graf är en mängd punkter, kallade noder, sammankopplade med linjer, kallade kanter. I en strukturell MR studie definierar man noderna utifrån de olika hjärnregionerna och kanterna utifrån associationerna mellan dessa regioner. Studien undersökte globala och lokala förändringar i nätverken hos friska individer med avvikande β-amyloid värden i ryggmärgsvätskan, då dessa personer anses löpa högre risk för att utveckla Alzheimer. Vår studie avslöjar att nätverksförändringar hos denna grupp kan påvisas redan innan enstaka volymförändringar kan detekteras.

Studier III och IV har som mål att undersöka huruvida vissa hjärnmetaboliter detekterade med MRS återspeglar en patologisk process specifik för Alzheimers sjukdom. Tidigare MRS studier har visat att ett Alzheimer-typiskt spektrum karakteriseras av en ökning i myoinositol (en organisk osmolyt) och en minskning av N-acetylaspartat (en neuronmarkör). Däremot finns det relativt lite kunskap kring samspelet mellan dessa förändringar och kända biomarkörer/riskfaktorer för Alzheimer. I **Studie III** undersöker vi det spektrala mönstret hos olika grupper som omfattar allt från friska äldre med normala β-amyloid värden till personer med lätta kognitiva störningar och avvikande β-amyloid (s.k. prodromal Alzheimer). Studien visar att koncentrationerna av myoinositol är förhöjda i det allra tidigaste skedet av det patologiska förloppet, dvs redan hos friska personer med lågt (avvikande) β-amyloid. **Studie IV** är till stor del en uppföljning av det föregående arbetet och den första longitudinella MRS studien där även β-amyloid analyseras. **Studie IV** påvisar att kopplingen mellan β-amyloid och myoinositol kvarstår över tid. Individer med ursprungligt låga β-amyloid värden ackumulerar myoinositol i en påtagligt högre takt. Sambandet mellan myoinositol och amyloidrelaterade patofysiologiska processer är ett spännande fynd som förhoppningsvis leder till att MRS kan få en bredare användning i samband med demensundersökningar och kliniska prövningar.

LIST OF SCIENTIFIC PAPERS

I. Voevodskaya O., Simmons A., Nordenskjöld, Kullberg, Ahlström H, Lind L, Wahlund LO, Larsson EM, Westman E; Alzheimer's Disease Neuroimaging Initiative. The effects of intracranial volume adjustment approaches on multiple regional MRI volumes in healthy aging and Alzheimer's disease.
Frontiers in Aging Neuroscience, 2014, 6, 264.

II. Voevodskaya O., Pereira JB., Volpe G., Lindberg O., Stomrud E., van Westen D., Westman E. and Hansson O. Altered structural network organization in cognitively normal individuals with amyloid pathology.
Neurobiology of Aging, 2017, 64, 15-24

III. Voevodskaya O., Sundgren PC., Strandberg O., Zetterberg H., Minthon L., Blennow K., Wahlund L-O., Westman E. and Hansson O. Myo-inositol changes precede amyloid pathology and relate to APOE genotype in Alzheimer disease.
Neurology, 2016, 86(19), 1754-1761

IV. Voevodskaya O., Poulakis K., Sundgren PC., van Westen, D., Palmqvist, S., Wahlund L-O., Stomrud E., Hansson, O. and Westman E.
Brain myo-inositol as a potential marker of amyloid-related pathophysiological processes: a longitudinal study.
Manuscript under review

CONTENTS

LIST OF ABBREVIATIONS

Aβ	Amyloid β
AD	Alzheimer's disease
ADAS-cog	Alzheimer's Disease Assessment Scale - cognitive subscale
ADNI	Alzheimer's disease neuroimaging initiative
APOE	Apolipoprotein E (gene)
APP	Amyloid precursor protein
BioFINDER	Biomarkers for Identifying Neurodegenerative Disorders Early and Reliably
Cho	Choline
CSF	Cerebrospinal fluid
CTL	Control subjects
DMN	Default mode network
DSM	Diagnostic and statistical manual of mental disorders
DTI	Diffusion tensor imaging
FDG	^{18}F-fluorodeoxyglucose
f-MRI	Functional magnetic resonance imaging
GM	Gray matter
ICV	Intracranial volume
ICD	International classification of diseases
LME	Linear mixed effects
MCI	Mild cognitive impairment
mI	Myo-inositol
MMSE	Mini-mental state examination
MRS	Magnetic resonance spectroscopy
MRSI	Magnetic resonance spectroscopic imaging
MRI	Magnetic resonance imaging
MTA	Medial temporal lobe atrophy
NAA	N-acetyl-aspartate
NFT	Neurofibrillary tangles
NIA-AA	National Institutes of Health and the Alzheimer's Association

PET	Positron emission tomography
PRESS	Point RESolved spectroscopy
P-tau	Phosphorylated tau
RF	Radio frequency
SCD	Subjective cognitive decline
SD	Standard deviation
SVS	Single-voxel spectroscopy
TE	Echo time
TR	Repetition time
T-tau	Total tau
WM	White matter
WMH	White matter hypointensities

1 INTRODUCTION

"Our memory is our coherence" wrote the revolutionary film-maker Luis Buñuel, "our reason, our feeling, even our action." (Buñuel, 1983). Our memories are so intricately intertwined with our identity, that any assault on these memories feels like a threat to our essence, our fundamental nature. Indeed, "I have lost myself" was the response frequently given by Auguste Deter, the first patient diagnosed with Alzheimer's disease (AD), to questions she could no longer answer (Maurer et al., 1997). Today, more than a hundred years later, it is still this vanishing sense of self that makes AD so frightening for patients and their loved ones. What's more, our ability to recall the past also plays a role in how well we can imagine the future. Being unable to retrieve past experiences compromises our ability to simulate potential future scenarios. This "imagination impairment" is a less talked about burden associated with AD (Schacter et al., 2012).

AD is the most common form of dementia, accounting for over two thirds of all dementia cases worldwide. One of the earliest and the most noticeable features of AD is the impairment of episodic memory – the memory system responsible for our ability to recall specific events of our past (Gold and Budson, 2008). As the disease progresses, cognitive decline becomes more prominent and starts to interfere with activities of daily living. People afflicted with AD usually develop symptoms in their late seventies, but we know today that the very first signs of pathology can be detected decades before symptom onset (Bateman et al., 2012; Buchhave et al., 2012). Since the asymptomatic "silent" phase of AD spans over many years, there is a great interest in characterizing the earliest disease stages. The studies included in this thesis aim to provide new insights on the changes taking place early on in the course of AD pathology.

1.1 ALZHEIMER'S DISEASE NEUROPATHOLOGY

The main hallmarks of AD were identified by Alois Alzheimer in 1906, when he described the characteristic silver-staining deposits in the cortex, and fibrillar bundles located at the site of disintegrated neurons (Stelzmann et al., 1995). These features would later become known as amyloid plaques and neurofibrillary tangles and are today considered essential for a definitive AD diagnosis.

The main constituent of the extracellular amyloid plaques is the fibrillar amyloid-β (Aβ) protein (Glenner and Wong, 1984; Masters et al., 1985). Aβ is derived through the cleavage of the APP protein by β- and γ-secretase enzymes. This pathway is sometimes referred to as amyloidogenic, or "pathological", as opposed to the non-amyloidogenic (physiological) pathway, during which no Aβ is generated. The 42-amino-acid-long isoform of Aβ (Aβ42) is the species most prone to fibrillization; it aggregates into oligomers, protofibrils, fibrils and finally forms Aβ plaques. An imbalance between the production and clearance of Aβ is thought to be a central event in AD (Hyman et al., 1993). Amyloid-β accumulation starts in the neocortex, propagating inward to allocortical structures, the diencephalon and the basal ganglia (Brettschneider et al., 2015). Although amyloid plaques are a trusted predictor of AD, their distribution does not correlate well with disease severity (Holmes et al., 2008). Instead,

overwhelming evidence places the toxic soluble Aβ oligomers at the core of AD pathogenesis (Benilova et al., 2012; Haass and Selkoe, 2007), suggesting that Aβ plaques are probably not harmful in and of themselves.

Neurofibrillary tangles (NFTs) are composed of the hypophosphorylated microtubule-associated protein tau (Grundke-Iqbal et al., 1986). In physiologic conditions, tau protein stabilizes axonal microtubules; the abnormal aggregation of tau into NFTs disrupts axonal transport and compromises synaptic activity (Iqbal et al., 2005). The NFTs are deposited inside the neurons, but when the neurons disintegrate completely, the NFTs remain at the site as "ghost tangles". In AD, the regional and temporal distribution of the NFTs is well described (Braak et al., 2006; Braak and Braak, 1991). Tangle deposition starts in the transentorhinal and entorhinal cortices, progressing to the hippocampus, finally spreading to the neocortex (Braak et al., 2006). Tau pathology follows a predictable pattern and is closely associated with the extent of neuronal loss and cognitive symptoms (Arriagada et al., 1992; Giannakopoulos et al., 2003; Gómez-Isla et al., 1997). Whether tangles actively contribute to neuronal death, or whether the formation of the NFTs constitutes the neurons' protective response to pathology, is not fully understood (Morris et al., 2011).

1.2 RISK AND PROTECTIVE FACTORS

1.2.1 Genetics

Familial AD – the hereditary form of the disease, usually strikes people before the age of 65 and is responsible for approximately 1-6% of AD cases. This form of autosomal dominant AD is caused by mutations in three genes: the presenilin 1 (*PSEN 1*) and presenilin 2 (*PSEN 2*) genes, and the β-amyloid precursor protein (*APP*) (Lynn et al., 2010). *APP* is located on chromosome 21, a trisomy of which is the cause Down's syndrome. Due to overexpression of APP, people with Down's syndrome develop typical characteristics of AD brain pathology (amyloid plaques and neurofibrillary tangles) by mid-life (Wiseman et al., 2015). Studies involving families afflicted with the familial form of AD, as well as individuals with Down's syndrome have been instrumental to our knowledge of AD pathogenesis.

The far more prevalent form of AD is the sporadic kind. Carriership of the ε4 allele of the APOE gene is the main known genetic risk factor for sporadic AD (Liu et al., 2013). APOE e4 affects the age of onset and the prevalence of the disease in a gene dose-dependent manner (Corder et al., 1993; Farrer et al., 1997). The risk of developing AD is 3-fold in heterozygous and 12-fold in homozygous ε4 carriers (Farrer et al., 1997). The e3 allele does not seem to be linked to AD pathogenesis, whereas the less common ε2 allele is in fact protective against the disease (Farrer et al., 1997). It is thought that APOE ε4 contributes to disease pathogenesis through promoting Aβ aggregation and deposition, as well as through Aβ-independent mechanisms such as compromised synaptic integrity and enhanced neuroinflammation (Kanekiyo et al., 2014; Liu et al., 2013). Neuroimaging studies have revealed that cognitively normal carriers of the ε4 allele display reduced hippocampal volumes, decreased glucose

metabolism and higher fibrillar Aβ burden compared to ε4 non-carriers (Reiman et al., 2009; Reiman et al., 1998).

1.2.2 Life style factors

Although genetics and heredity studies are invaluable for our understanding of the disease, recent research suggests that lifestyle settings and choices may play a bigger role in AD than what was previously thought. Areas where constructive changes can potentially be made, the so-called modifiable risk factors of AD, are strikingly similar to known cardiovascular risk factors and include obesity, hypertension, diabetes mellitus, high cholesterol and smoking (deBruijn et al., 2015; Kivipelto et al., 2005) Indeed, many of the recent lifestyle, nutrition and exercise interventions are proving evidence for the "good for your heart, good for your brain" hypothesis (Ngandu et al., 2015; Sindi et al., 2015).

1.2.3 Cognitive reserve

The concept of cognitive reserve is based on the evidence that some people can tolerate more pathological brain changes than others until they develop symptoms. This can perhaps be attributed to actual inter-individual differences in brain size, but it is more likely that this "resilience" to neurodegenerative processes stems from educational and occupational experiences (Stern, 2012). It has consistently been demonstrated that complex patterns of mental activity throughout life are associated with lower incidence of dementia (Valenzuela and Sachdev, 2006). Furthermore, a longitudinal study showed that an intellectually enriched lifestyle may have the potential to delay dementia onset (Vemuri et al., 2014).

1.3 FROM NORMAL AGEING TO ALZHEIMER'S DISEASE

1.3.1 Normal ageing

As we get older, our brain is subjected to structural and functional changes. Understanding the effects of healthy ageing on the brain and cognition is important to identify and isolate the contribution of pathology. As the brain ages, it suffers from volume loss, with annual decreases in gross brain volume at a rate of approximately 0.5% per year (Fjell et al., 2014). Notably, the typical changes associated with AD pathology, such as cortical thinning and reductions in hippocampal volume also belong to the most prominent changes associated with healthy ageing. Reductions in cortical thickness seen in normal ageing most probably arise from the loss of synapses and compromised dendritic structure, rather than neuronal death (Harada et al., 2013).

When it comes to the main areas of cognitive decline associated with normal ageing, these are related to processing speed (the speed with which one carries out mental tasks), as well as memory and executive function (Deary et al., 2009). Episodic memory, one of the domains affected very early in AD, also deteriorates in healthy ageing (Fjell et al., 2014).

1.3.2 Subjective cognitive decline

The subjective cognitive decline (SCD) framework was established to identify the very first clinical manifestations of AD, in cases where no objective cognitive deficit is detected (Jessen et al., 2014). Elderly people frequently report a worsening of cognitive abilities. This self-perceived cognitive decline over time together with normal performance on neuropsychological tests (adjusted for age and education level) warrant the clinical diagnosis of SCD (Jessen et al., 2014). It has been shown that SCD is associated with a higher risk of developing mild cognitive impairment and conversion to dementia (Mitchell et al., 2014). Although SCD may represent the earliest stage of disease, it is important to recognize that the term SCD deals with a fundamentally heterogeneous population. This is due in part to the subjective nature of the "self-report", and in part to the overlap between SCD and some aspects of depression and anxiety (Hill et al., 2016).

1.3.3 Mild cognitive impairment

Mild cognitive impairment (MCI) denotes the intermediate clinical state between normal ageing and a dementia diagnosis (Petersen et al., 1999). MCI can manifest itself as amnestic– associated with memory impairment, and non-amnestic – characterized by decline in non-memory domains (Petersen, 2004). In 2011 the National Institute on Aging and Alzheimer's Association (NIA-AA) workgroup set out to establish a set of clinical and research criteria for "MCI due to AD", in order to better characterize the symptomatic predementia stage of AD (Albert et al., 2011). The *clinical criteria* are designed to be used broadly in all clinical settings and do not require access to specialized procedures or biomarkers. The *research criteria* incorporate the use of AD biomarkers, namely markers reflecting cerebral amyloidosis and neuronal injury, allowing for an "MCI due to AD" diagnosis to be made with different degrees of certainty.

MCI is an important diagnostic entity for AD research for several reasons: 1) it encompasses a large population, with a prevalence of 15%-20% among people above 65 (Mariani et al., 2007; Petersen et al., 2010), 2) it identifies individuals at high risk of progressing to dementia, with conversion rates of 10-15% per year in clinical studies and 5-10% per year in population-based studies (Mariani et al., 2007) and 3) neuropathologically, it represents a stage intermediate between physiological ageing and AD (Petersen et al., 2006).

1.3.4 Alzheimer's disease clinical features and diagnostic criteria

Clinical progression of AD can be divided into three stages – mild, moderate and severe. The mild stage is accompanied by a deterioration of episodic memory, mood changes and a decline in reasoning and judgement. During the moderate stage, the impairment of other cognitive abilities such as language, attention and orientation advances along with the progressive loss of memory. In severe AD, speech and vision become compromised (McKhann et al., 2011). The clinical manifestation of AD as well as the speed at which the disease progresses vary somewhat between patients. There is also evidence of there being distinct clinicopathological subtypes within the diagnosis of AD (Ferreira et al., 2017; Murray et al., 2011). The

phenomenon of AD subtypes may at least in part explain the heterogeneity of the clinical picture of the disease.

For a clinical diagnosis of probable AD, the most commonly used criteria were defined by the National Institute of Neurological and Communicative Disorders and Stroke and Alzheimer's Disease and Related Disorders Association (NINCDS-ADRDA) (McKhann et al., 1984). In 2011, a new set of criteria was presented by the NIA-AA, where the use of biomarkers was incorporated into the diagnostic criteria (McKhann et al., 2011). Although the prevailing view is that a definitive diagnosis of AD can only be made using histopathological evidence at autopsy, it is important to recognize that a combination of family/informant history, neuropsychologic battery, imaging and fluid biomarkers can support an AD diagnosis to a high degree of certainty.

Another major set of diagnostic criteria was proposed by the International Working Group (IWG) in 2007 and revised in 2014 (IWG-2) (Dubois et al., 2014). According to the IWG-2 criteria objective memory impairment and positive biomarker evidence are mandatory for an AD diagnosis. In routine clinical practice, AD is usually diagnosed using the 4th edition of the Diagnosis and Statistical Manual of Mental Disorders (DSM-IV) and the 10th edition of the International Classification of Diseases (ICD-10).

1.4 ALZHEIMER'S DISEASE BIOMARKERS: DETECTING AND TRACKING PATHOLOGY

The term biomarker refers to a measurable indicator, signaling the presence of a medical condition. Such indicators are widely used in research and in the clinic to distinguish between normal physiological processes and pathology, as well as to evaluate the response to therapeutic interventions (Strimbu and Tavel, 2010). AD biomarkers provide scientists across the field with a common framework for conducting research and reporting findings. This universal language is also essential for defining disease staging and establishing inclusion/exclusion criteria for clinical trials (Hampel et al., 2010; Jack et al., 2011; Jack et al., 2016). In the field of AD, as well as in other areas of medical research, biomarkers must first of all be accurate and reproducible. Other qualities that one strives for in a successful biomarker are non-invasiveness, cost-efficiency, and the ability to detect the disease at the earliest possible stages.

In fact, a recently proposed "research framework to investigate the Alzheimer's disease continuum" puts forward the idea that an AD diagnosis should be based entirely on biomarkers, irrespective of clinical symptoms (Jack et al., 2016).

1.4.1 Neuroimaging

Advanced imaging modalities such as magnetic resonance imaging (MRI) and positron emission tomography (PET) allow researchers to investigate brain morphology, function and pathology *in vivo*. Neuroimaging is increasingly being used in disease diagnosis, for monitoring treatment effects, and will undoubtedly play an important role in the emerging field of personalized medicine. The choice of brain imaging technique is influenced not only by the

primary research (or medical) question, but also by more practical factors, such as cost, complexity and availability of the technique.

Basic principles of magnetic resonance

The phenomenon of nuclear magnetic resonance (NMR) arises from the magnetic properties of certain atomic nuclei.

Due to the intrinsic spin of the proton, hydrogen atoms in an external magnetic field precess about $\mathbf{B}_0$ with a characteristic Larmor frequency:

$$\omega = \gamma \boldsymbol{B}_0 \qquad (1.1)$$

where γ is the gyromagnetic ratio. The protons in a magnetic field assume one of two possible orientations, occupying the lower energy spin up level, parallel with $\mathbf{B}_0$ (β state) or the higher energy spin down level, antiparallel with $\mathbf{B}_0$ (α state). The energy difference between these states is ΔE; the frequency associated with this energy lays in the radio frequency (RF) band (Figure 1).

Nuclear spins do not populate the available energy levels evenly. Slightly more spins occupy the lower energy state α and the population follows the Boltzmann distribution:

$$\frac{N_\alpha}{N_\beta} = e^{(E_\beta - E_\alpha)/k_b T} \qquad (1.2)$$

When an RF pulse near the Larmor frequency is transmitted to the spin system, the spins transition from level α to level β. The energy emitted during the spin relaxation generates the MR signal. The intensity of the signal is proportional to the ratio of the number of protons in α and β states.

Macroscopically, the excess in the number of spins in the lower energy α state compared to the number of spins in the β state creates a net magnetization **M**, aligned with the direction of $\mathbf{B}_0$. Resonance condition is achieved when an electromagnetic RF pulse is applied perpendicularly to $\mathbf{M}_z$, to match the energy ΔE. When this 90° pulse is applied, the bulk magnetization vector **M** is tipped onto the transverse xy-plane, such that $\mathbf{M}_{total} = \mathbf{M}_{transverse}$. After the transmission is stopped, relaxation begins, and the magnetization vector splits into a transverse and a longitudinal component. Longitudinal relaxation (T_1), also known as spin-lattice relaxation, describes the return of the longitudinal magnetization $\mathbf{M}_z$ after a perturbation. Transverse relaxation (T_2), describes the loss of coherence by the spins, and is also known as spin-spin relaxation. Another relaxation process is described by T_2^* - the transverse relaxation time which takes into account inhomogeneities in $\mathbf{B}_0$ that further speed up the dephasing of the spins. (Figure 1). The precession of the net magnetization vector generates an oscillating electromagnetic field, which induces a current in the receiver coil. This signal, the Free Induction Decay, decreases as a result of the loss of phase coherence. Finally, this observable time domain signal is converted into the frequency domain using the Fourier transform (Figure 1).

Depending on their local chemical environment, hydrogen atoms of different molecules experience slightly different magnetic fields. This happens because the electrons, surrounding the hydrogen nuclei shield them slightly from the external magnetic field. The extent of this shielding depends on the structure and conformation of the molecule generating the signal. As a result, the effective magnetic field "felt" by the protons amounts to $\mathbf{B}_0(1-\sigma)$, where σ is the shielding constant; and the associated frequency is

$$\omega_s = \gamma B_0(1-\sigma) \qquad (1.3)$$

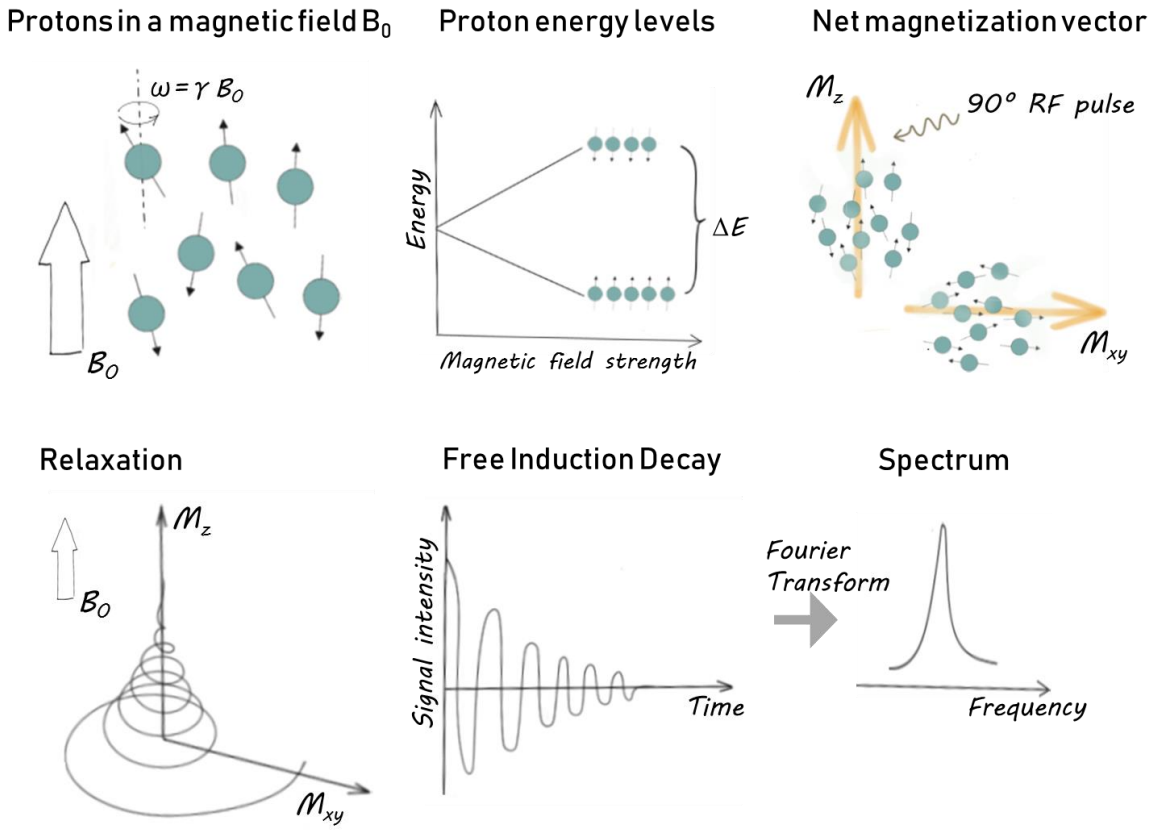

Figure 1 | Illustration of the principles of MR spectroscopy

Since different molecules resonate at slightly different frequencies, we can identify the constituents of organic compounds from their distinct spectral "fingerprints". From Equation 3 follows that the frequency shift between nuclei in different chemical environments becomes greater at increasing magnetic field strengths, leading to more spatially resolved resonance peaks. MRS is a technique which benefits greatly from being conducted at higher field strengths, since the improved resolution allows identification of a larger number of metabolites. In Figure 2, an example of a high-resolution spectrum collected from the rat brain and its constituent individual metabolite profiles is presented.

MR spectra can be acquired using different localization techniques. In single-voxel-spectroscopy (SVS), the signal is acquired from a single volume in the brain. The selection of the voxel of interest (typically ≈1-2 cm^3) is achieved by applying mutually orthogonal slice selective gradient pulses, so that only the signal from the protons within this restricted volume

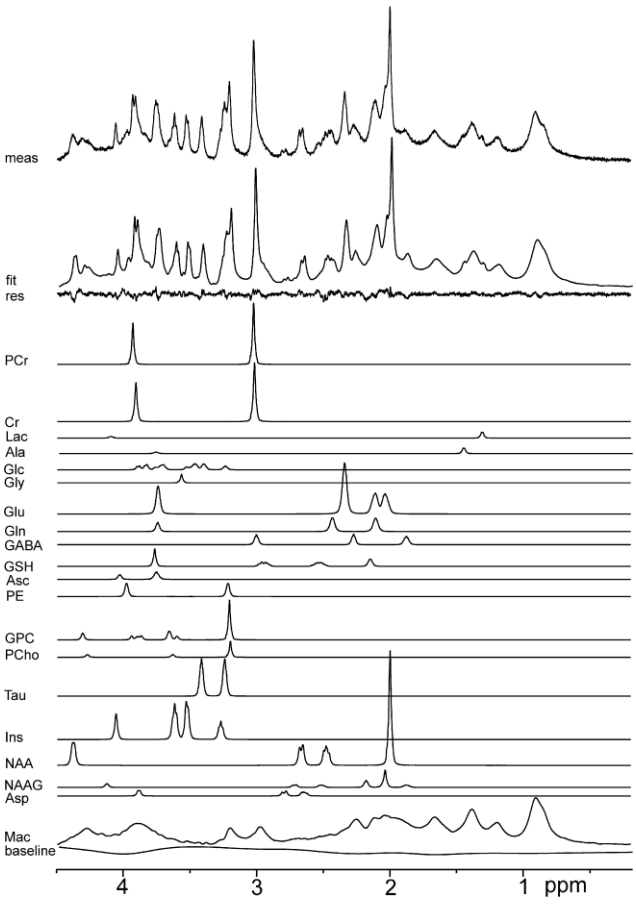

Figure 2 | Decomposing the MR spectrum. From the top, MRS of the rat brain at 14.1 T, followed by the LCModel fit, the residual spectrum and the fits of individual metabolites. Reproduced from Mlynárik et al (Mlynárik et al., 2008) with permission from Elsevier

is picked up. This method allows for a selection of a physiologically relevant volume of interest, and the optimization of the homogeneity of the magnetic field across this volume. Another localization technique involves collecting signal from multiple voxels (≈5 mm^3) at a time. This method, referred to as MRS imaging (MRSI), generates spectra from a multidimensional array of regions, creating spatial maps of different metabolites. MRSI has the advantage of being able to characterize an entire object, rather than a selected volume of interest. However, it is also a more methodologically demanding technique, as homogeneity of the B field is more difficult to achieve and the inherent acquisition times are longer.

The process of how an MR image is created is not covered in detail in this thesis. In brief, the generation of a two-dimensional MR image is based on the phenomenon of NMR relaxation described earlier. T_1 and T_2 relaxation times differ depending on the chemical composition or physiological status of biological tissues, allowing T_1 and T_2 weighted images to reveal contrast between different types of matter in the brain. Using the gradient coils of an MRI scanner, local variations in the magnetic field are generated in any linear combination of the x, y and z directions. The slice selective, frequency encoding and phase encoding gradients allow for a 2D image to be reconstructed from a one-dimensional signal.

MRI in Alzheimer's disease: Imaging atrophy

Neurodegeneration is a general term used to describe progressive deterioration of the structure and function of neurons. Macrostructurally, the loss of brain tissue (atrophy) can be tracked using structural MRI. Assessing the extent of brain atrophy, particularly in the medial temporal lobe, is an important part of the diagnostic work up in patients with dementia.

The pattern of brain atrophy overlaps with the topography of tangle deposition (Whitwell et al., 2008) and largely reflects the extent and progression of cognitive deficits (Frisoni et al., 2010). The earliest and most severe atrophic changes occur in the entorhinal cortex and the

hippocampus, propagating to the temporoparietal association cortices and then to the neocortical areas (Thompson et al., 2003).

There are several ways in which structural MR information can be used as a disease biomarker. Hippocampal volumes and whole-brain atrophy rates can – independently or together with other AD biomarkers – help identify individuals who are likely to progress to dementia (Apostolova et al., 2006; Jack et al., 1999; Spulber et al., 2010; Walhovd et al., 2010). Structural information is also an integral part of differential diagnosis. Dementias of etiologies other than AD include: Lewy bodies and vascular dementia, where medial temporal lobe atrophy is almost absent; fronto-temporal lobe dementia, characterized by atrophy in the frontal lobe; semantic dementia, where the medial temporal lobe atrophy is clearly asymmetrical (Vemuri and Jack, 2010). Further, MRI measures are useful for clinical trials, for 1) screening for inclusion/exclusion criteria, 2) quantifying disease progression and the effect of disease-modifying interventions (Fox et al., 2000; Vemuri and Jack, 2010).

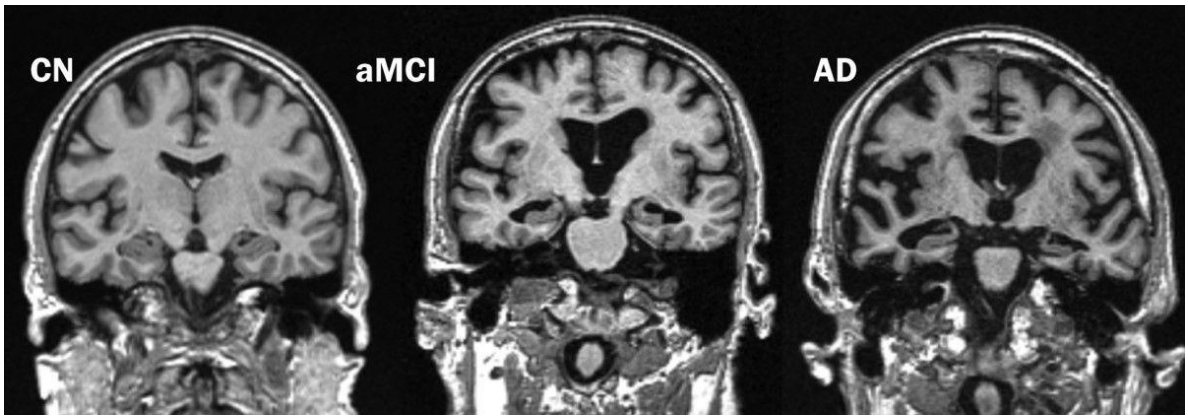

Figure 3 | Medial temporal lobe atrophy in an older cognitively normal individual (CN), a patient with amnestic MCI (aMCI) and Alzheimer's disease (AD). As originally published by Biomed Central in (Vemuri and Jack, 2010).

MRS in Alzheimer's disease: Exploring biochemistry

N-acetyl-aspartate (NAA) is a marker of neuronal integrity that is decreased in patients with AD compared to cognitively healthy older adults (Kantarci, 2013). *In vivo* brain NAA levels are closely linked to neuronal energetics, where NAA has been proposed to reflect impaired mitochondrial function, in addition to being a marker of neuronal cell density (Bates et al., 1996; Jessen et al., 2011; Murray, M. E. et al., 2014). A decrease in NAA levels is often not seen in early stages of AD, but progresses with increasing disease severity (Adalsteinsson et al., 2000). NAA levels have also been shown to decrease proportionally to the extent of damage to the brain, for example in traumatic brain injury (Signoretti et al., 2008). In patients with MCI or AD, NAA declines with progressing dementia severity (Huang et al., 2001; Kantarci, 2013).

Myo-inositol (mI) is emerging as probably the most relevant MRS metabolite in the context of AD. The physiological role of mI is that of an organic osmolyte (Kwon et al., 1992); intracellular mI concentrations increase as a response to extracellular hypertonicity (Lee et al., 1994) and decrease in hypotonic conditions (Videen et al., 1995). Furthermore, mI elevation

seems to be related to Aβ plaque pathology, i.e. higher baseline levels of mI are associated with increased Aβ accumulation over time (Nedelska et al., 2017). Brain mI is elevated at pre-dementia stages of Down syndrome (Huang et al., 1999) and familial AD (Godbolt et al., 2006), and ante-mortem mI levels are associated with post-mortem cored and diffuse amyloid plaques (Murray, M. E. et al., 2014). It has been suggested that mI may be a potential marker of glial proliferation (Bitsch et al., 1999), however the utility of mI as an indicator for the degree of inflammation in AD is unclear (Maddock and Buonocore, 2012; Murray, Melissa E. et al., 2014).

Choline (Cho) is composed of phosphorylcholine and glycerophosphorylcholine – both products of cellular membrane breakdown (Klein, 2000). Although Cho is known to indicate membrane turnover, its significance in AD pathology is not fully understood.

Total **creatine (Cr)**, a resonance peak composed of creatine and phosphocreatine is essential of energy storage and transfer (Rackayova et al., 2017), and is often used as an internal reference in spectroscopy studies.

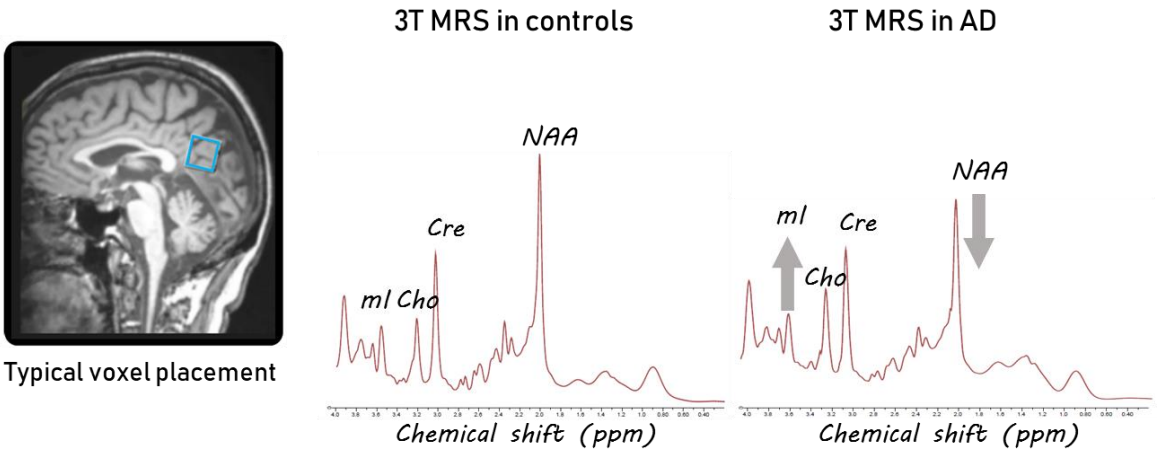

Figure 4 | Illustration of MRS in AD. Voxel placement in the precuneus / posterior cingulate.

Intracranial volume in volumetric MRI

In volumetric studies of neurodegeneration, the intracranial volume (ICV) provides an estimate of premorbid brain size. The assumption is that the ICV, unlike total brain volume, remains unchanged in both normal and pathological ageing (Blatter et al., 1995).

Although the relationship between premorbid brain volume and the onset of disease in later life has been studied explicitly (Graves et al., 1996; Jenkins et al., 2000; Tate et al., 2011), for most imaging studies of neurodegeneration ICV is a nuisance variable that may complicate interpretation of the results. Regional brain volumes scale with head size, therefore inter-individual variability of the ICV may mask or exaggerate true structural differences.

Several approaches can be used to account for the effects of ICV on regional brain volumes. There is no unified approach for ICV correction in morphological MRI studies and the choice is usually one of the following methods: 1) describing each volume as a proportion of the ICV,

2) using the residuals of a linear regression to remove all association between regional volumes and the ICV, 3) including the ICV as a covariate in an analysis of variance model. These approaches are addressed in more detail in the Methods section.

Positron emission tomography

Amyloid positron emission tomography (PET) allows *in vivo* quantification of Aβ burden. Amyloid-specific tracers used clinically and in research (Pittsburgh Compound B, Flutemetamol etc) are compounds characterized by having a high affinity for the insoluble fibrillar Aβ deposits. Cortical retention of an amyloid tracer follows the pattern of regional distribution of Aβ plaques, with higher plaque density in the frontal and anterior cortex, cingulate gyrus and precuneus (Ikonomovic et al., 2008). However, plaque distribution does not correlate well with disease severity (Holmes et al., 2008).

Recent advances in the development of tau-specific PET tracers have yielded the possibility of imaging tau pathology in vivo. The pattern of pathological tau aggregation is related to the clinical presentation of AD (Ossenkoppele et al., 2016). Future findings from tau PET studies may be able to answer important questions about fundamental disease mechanisms.

Another application of PET in the context of AD, is imaging metabolic activity through measuring regional glucose uptake using the [^{18}F]fluoro-2-deoxy-D-glucose (FDG) tracer, allowing indirect quantification of neuronal activity and synaptic density (Mosconi, 2013).

1.4.2 Cerebrospinal fluid markers

CSF levels of Aβ42, total tau (T-tau) and phosphorylated tau (P-tau) are routinely measured in AD, both in order to identify the disease at its earliest stage as well as for differential diagnosis (Olsson et al., 2016). These markers reflect the fundamental aspects of AD pathogenesis – the formation of plaques, neuronal degeneration and tangle formation (Blennow and Hampel, 2003). Reductions in CSF Aβ42 levels can be detected up to 15 years before symptom onset (Bateman et al., 2012), making Aβ42 the earliest biomarker to become abnormal in AD. Importantly, early changes in Aβ42 alone are not specific to AD, however when detected together with increases in T-tau and P-tau are said to constitute the "AD signature" (Blennow et al., 2015). CSF t-tau reflects the extent of neuronal and axonal degeneration in the brain, with high levels of t-tau being linked to a steeper disease progression (Blom et al., 2009; Samgard et al., 2010), whereas levels of p-tau are likely to indicate tau phosphorylation and tangle formation (Blennow et al., 2015).

Apart from Aβ42, other isoforms of Aβ, such as Aβ40 and Aβ38 are present in the CSF. There is evidence supporting the use of Aβ42/Aβ40 ratio as an AD biomarker, since it has been shown to be a superior predictor of cortical amyloid accumulation and performed better in discriminating AD from other neurodegenerative disorders such as dementia with Lewy bodies and Parkinson's disease dementia (Janelidze et al., 2016).

1.4.3 Graph theory

A graph is a mathematical description of interconnected elements. Applying the graph theoretical framework to brain networks implies representing the anatomical regions as nodes and the connections between these nodes as edges. In the context of structural MR, the nodes of a network may be represented by segmented/parcellated brain regions, and the connections are the structural covariance measures between them. A set of network properties is commonly assessed in neuroimaging graph theory studies. *Global efficiency* is a measure of integration that provides information about the network's ability to rapidly incorporate information from distinct nodes of a network. *Clustering*, *transitivity* and *modularity* are segregation measures that indicate how strongly a network is locally interconnected or organized into different modules. *Hubs* are the central regions of a network that regulate the flow of information (Rubinov and Sporns, 2010) (See Figure 5 for an overview).

Network-based techniques are being successfully applied to neuroimaging data to uncover information about normal and pathological conditions undetectable by conventional morphometric studies. Several studies have explored disruptions in structural and functional networks occurring in AD (Dai and He, 2014; He et al., 2008; Pereira et al., 2015; Tijms et al., 2013; Yao et al., 2010). The most consistent findings in AD involve a decline in the ability to integrate information and a decrease in the number of hubs (Dai and He, 2014).

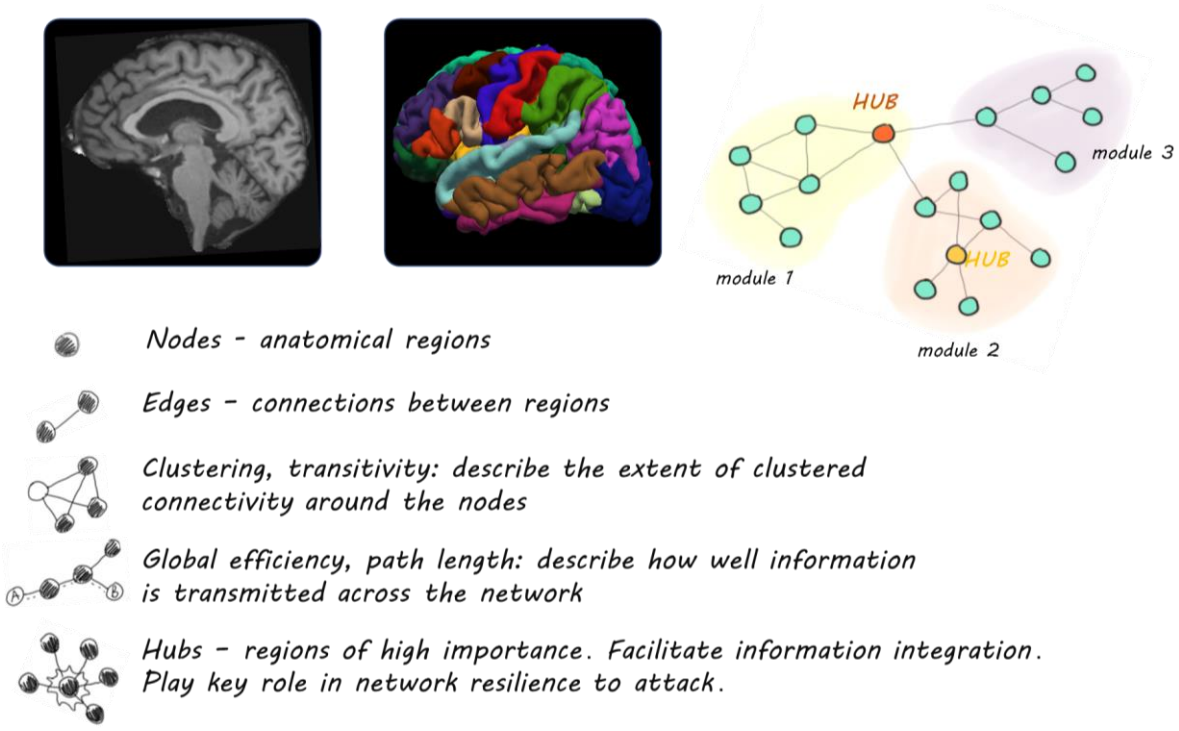

Figure 5 | Overview of basic graph theoretical concepts.

2 AIMS

This thesis aims to advance the characterization of the earliest stages of AD and provide new insights on the role of magnetic resonance spectroscopy as a potential disease biomarker. Studies I and II address the phenomenon of structural covariance in MR imaging. Studies III and IV explore the relationship between magnetic resonance spectroscopy markers and the pathological hallmarks of AD. Specifically:

In **Paper I** we investigate the implications of intracranial volume adjustment approaches on multiple regional MRI volumes in cognitively normal elderly, individuals with MCI and AD.

In **Paper II**, we examine whether the changes in the organization of structural brain networks are associated with amyloid pathology in cognitively normal elderly.

In **Paper III**, we investigate whether the levels of MRS metabolites are changed during preclinical AD, putting these alterations into the context of amyloid and tau pathology.

In **Paper IV**, we explore the association between longitudinal changes in MRS metabolites and amyloid pathology in non-demented individuals.

3 PARTICIPANTS AND METHODS

3.1 ETHICAL CONSIDERATIONS

All studies were conducted according to the Declaration of Helsinki and subsequent revisions. Study I was approved by the regional ethics committee in Uppsala, Sweden. The ADNI ethical approval was granted by the institutional review boards of the participating centers. Studies II-IV were approved by the regional ethics committee in Lund, Sweden. [18F]-flutemetamol PET imaging in Study III was approved by the Swedish Medicines and Products Agency and the local Radiation Safety Committee at Skåne University Hospital, Sweden.

3.2 PARTICIPANTS

A general overview of the cohorts and participant groups used in this thesis is presented in Figure 6 and Panel 1 of the Methods section.

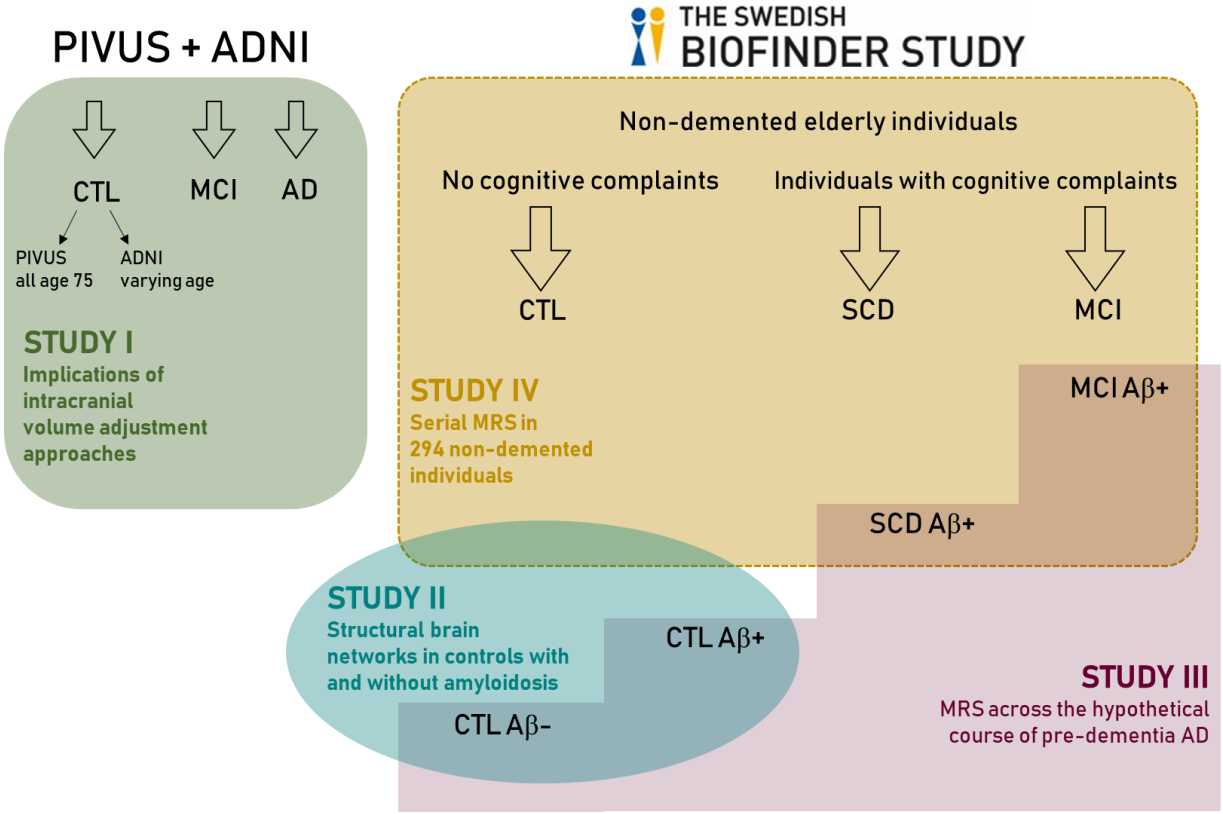

Figure 6 | Overview of the participant groups and research cohorts used in this thesis.

3.2.1 Study I participants

Data from two research cohorts, the PIVUS and the ADNI were used.

1) PIVUS: healthy controls, N=406
2) ADNI: healthy controls, N=223
3) ADNI: MCI, N=325
4) ADNI: AD, N=176

The PIVUS (Prospective Investigation of Vasculature in Uppsala Seniors) cohort (Lind et al., 2006) is a single-center community-based cohort of individuals residing in Uppsala, Sweden, primarily aimed at studying cardiovascular health. The neuroimaging aspect of the PIVUS study is unique in that the MRI scans were acquired at age 75 for all participants. The PIVUS study was approved by the local ethics committee. More information about the PIVUS cohort can be found on the study homepage http://www.medsci.uu.se/pivus/.

Table 1 | Demographics of the single-center epidemiological PIVUS cohort

	Female	Male	All
Number of participants	193	213	406
ICV, mm^3	1440320 (121240)	1638419 (140237)	1544249 (140237)
MMSE	28.8 (1.3)	28.5 (1.5)	28.7 (1.4)
Education			
< 9 years	58%	58%	58%
9-12 years	18%	20%	19%
> 12 years	24%	22%	23%
Age		75	

Values are reported as mean (SD); ICV= Intracranial volume; MMSE= Mini-Mental State Examination.

The ADNI (The Alzheimer's Disease Neuroimaging Initiative) is a multi-center study, launched in 2003 across North America with the overall goal to validate biomarkers for early detection and monitoring of AD pathology. Patients were diagnosed as having probable AD or MCI according to established criteria (McKhann et al., 1984; Petersen et al., 1999). More information about the ADNI can be found on at adni.loni.usc.edu.

Table 2 | Demographics of the subset of the multi-center ADNI cohort

	CTL			MCI	AD
	Female	Male	All	All	All
Number of participants	107	116	223	325	176
ICV, mm^3	1444626 (120830)	1617014 (134231)	1534299 (157978)	1565894 (166451)	1532681 (175643)
MMSE	29.2 (1.0)	29.0 (1.0)	29.1(1.0)	27.1(1.8)	23.3(2.0)
Education					
< 9 years	2%	2%	2%	2%	5%
9-12 years	15%	4%	9%	17%	27%
> 12 years	83%	94%	89%	81%	68%
Age	76.1 (4.8)	75.8 (5.3)	75.9 (5.1)	74.5 (7.1)	75.1 (7.3)

Data for ICV, MMSE and age presented as mean (standard deviation); ICV= Intracranial volume; MMSE=Mini-Mental State examination

3.2.2 Study II-IV

In studies II-IV, data from the BioFINDER cohort was used. The Swedish BioFINDER (*Biomarkers for Identifying Neurodegenerative Disorders Early and Reliably)* study is a prospective longitudinal multi-center study aimed at discovering novel AD biomarkers. The BioFINDER is composed of cognitively healthy participants (CTL), individuals with subjective cognitive decline (SCD) and mild cognitive impairment (MCI). More information,

such as the details of inclusion/exclusion criteria is available on the study homepage www.biofinder.se and papers II-IV.

Study II participants

In Study II, only participants with no form of cognitive complaints (the CTL subset) of the BioFINDER were included. The groups contrasted in this study were based on a CSF Aβ42/Aβ40 (cut-off at 0.1) and included:

1) healthy controls with normal (negative) CSF Aβ42/Aβ40, N=233
2) healthy controls with abnormal (positive) CSF Aβ42/Aβ40, N=66

Table 3 | Demographics of the study sample used in Study II

	CSF Aβ- Aβ42/Aβ40 > 0.1 N =233	CSF Aβ+ Aβ42/Aβ40 ≤ 0.1 N = 66
Gender (female/male)	137/96	44/22
Age, years	72.9 (5.0)	74.9 (4.8)
APOE genotype (% ε4 carriers)	19%	46%
Years of education	12.2(3.4)	12.2(4.7)
Cognitive measures		
MMSE	29.0 (1.0)	29.0 (0.8)
AQT	66.5 (13.1)	66.8 (12.8)
ADAS-cog	1.9 (1.8)	2.6 (2.4)
CSF Aβ42/Aβ40	0.14 (0.03)	0.07 (0.01)

ADAS-cog = Alzheimer's Disease Assessment Scale–cognitive; AQT = A Quick Test of Cognitive Speed; MMSE = Mini-Mental State Examination. Values are reported as mean (SD).

Study III participants

In Study III, we aimed to select participant groups that mimic the hypothetical course of AD progression, based on their CSF Aβ42 (cut-off at 530 ng/L) levels. This resulted in the following four groups:

1) healthy controls with normal (negative) CSF Aβ42, N=156
2) healthy controls with abnormal (positive) CSF Aβ42, N=59
3) individuals with SCD with abnormal (positive) CSF Aβ42, N=49
4) individuals with MCI with abnormal (positive) CSF Aβ42, N=88

Table 4| Demographics of the study sample used in Study III

	CTL Aβ42- CSF Aβ42 > 530 ng/L N =233	CTL Aβ42+ Aβ42 ≤ 530 ng/L N =59	SCD Aβ42+ Aβ42 ≤ 530 ng/L N =49	CSF Aβ42+ Aβ42 ≤ 530 ng/L N =88
Gender (female/male)	95/61	36/23	27/22	43/45
Age, years	72.6 (4.7)	72.7 (4.7)	70.7 (5.7)	71.7 (5.2)
APOE genotype (% ε4 carriers)	18%	61%	71%	74%
Years of education	12.1(3.7)	11.7(3.8)	12.1(3.8)	11.6(3.3)
Cognitive measures				
MMSE	29.1 (0.9)	29.2 (0.9)	28.0 (1.6)	26.9 (1.7)
AQT	66.1 (12.5)	66.1 (11.6)	76.2 (18.5)	90.1 (31.1)
ADAS-cog	1.6 (1.6)	2.2 (2.3)	3.9 (2.1)	7.1 (1.9)
CSF Aβ42, ng/L	753 (127)	416 (75)	384 (79	359 (84)
CSF tau, ng/L	125 (63)	164 (103)	231 (95)	209 (100)
CSF p-tau, ng/L	51 (15)	58 (25)	77 (31)	74 (36)
PET (PCC/precuneus)	1.26 (0.15)	1.74 (0.41)	1.96 (0.40)	2.19 (0.47

ADAS-cog = Alzheimer's Disease Assessment Scale–cognitive; AQT = A Quick Test of Cognitive Speed; MMSE = Mini-Mental State Examination, PCC=Posterior Cingulate Cortex. Values are reported as mean (SD).

Study IV participants

In Study IV, we were interested in data from individuals for whom baseline CSF was available, and who had at least one MRS follow-up. This resulted in the following groups:

1) healthy controls, N=137
2) individuals with SCD, N=83
3) individuals with MCI, N=74

Table 5 | Demographics of the study sample used in Study IV.

	CTL N = 137	SCD N = 83	MCI N = 74
Sex (male/female)	57/80	36/47	41/33
Age, years	72.8 (4.7)	70.2 (5.5)	69.9 (4.9)
CSF Aβ42 status: Normal/abnormal (< 530 ng/L)	98/33	51/30	25/48
APOE genotype: (% of ε4 carriers)	30%	40%	54%
Years of education	12.3 (3.6)	13.1 (3.6)	11.6 (3.4)
MMSE (baseline)	29.0 (1.0)	28.5 (1.5)	27.5 (1.8)
MMSE 2 year follow-up	28.9 (1.7)	28.4 (2.7)	25.3 (3.5)
MMSE 4 year follow-up	28.6 (1.7)	27.3 (4.3)	23.5 (3.9)

MMSE = Mini-Mental State Examination Values are reported as mean (SD).

3.3 METHODS

3.3.1 MRI image acquisition and processing (Studies I-II)

Image acquisition: MRI protocol

T1-weighted MR images were acquired as part of all the constituent studies. However, structural data was used explicitly only in studies I and II.

PIVUS: MR images were acquired on a 1.5 Tesla MRI scanner (Philips Healthcare, Best, The Netherlands) and included a sagittal T1-weighted 3D gradient echo sequence (echo time: 4.0ms, repetition time: 8.6ms, resolution: $0.94\times0.94\times1.2mm^3$). All images were reviewed according to previously published quality control criteria (Simmons, 2011; Simmons et al., 2009).

ADNI: MR images were collected from several 1.5 Tesla systems, including a high resolution sagittal 3D T1-weighted MPRAGE sequence (echo time 4.0 ms, repetition time: 9ms, resolution $1.1\times1.1\times1.2mm^3$). The quality of the MPRAGE images was assessed by the ADNI MRI quality control center at the Mayo Clinic (Rochester, MN) according to standardized criteria.

BioFINDER: MR images were collected on a single 3 Tesla systems (Trio, Siemens, Germany) and included a 3D T1-weighted MPRAGE sequence (echo time 3.4 ms, repetition time: 1950 ms, $1.1\times1.0\times1.0mm^3$).

Image processing: FreeSurfer pipeline

The FreeSurfer pipeline estimates regional cortical thickness and volumetric measures from T1 3D brain MRI scans. The software is documented and freely available at http://surfer.nmr.mgh.harvard.edu/. In the cortical (surface-based) stream, Freesurfer models the boundary between white matter and gray matter, as well as the boundary between gray matter and the pial surface, to estimate cortical thickness and describe cortical folding patterns. In the subcortical (volume-based) stream, automatic segmentation is performed to label deep gray matter volume structures (Fischl et al., 2002; Fischl et al., 2004), such as the hippocampus, amygdala, caudate, putamen, ventricles etc.

In brief, the processing steps are: removal of non-brain tissue (skull-stripping) (Segonne et al., 2004), Tailarach transformation, segmentation of the subcortical white matter and deep gray matter volumetric structures (Fischl et al., 2002; Fischl et al., 2004), intensity normalization (Sled et al., 1998), tessellation of the gray-white matter boundary, correction of topology (Segonne et al., 2007) and an adjustment of the localization of tissue borders (Fischl and Dale, 2000). Upon the creation of cortical models, each subject surface is registered to a spherical atlas based on the individual cortical folding patterns (Fischl et al., 1999). This is followed by parcellation of the cerebral cortex into cortical regions specified by an atlas, from which cortical thickness and volume measures can be extracted. The Desikan altas (68 cortical regions) has been used throughout this thesis (Desikan et al., 2006).

	Study I ADNI+PIVUS	Study II BioFINDER	Study III BioFINDER	Study IV BioFINDER
Main theme	Structural covariance		Magnetic resonance spectroscopy	
Specific theme	Intracranial volume adjustment approaches in volumetric MR studies	Structural network topology and amyloid pathology	Interplay between MRS metabolites and existing clinical and pathological AD biomarkers	The relationship between longitudinal change in MRS metabolites and amyloid pathology
Study design	Cross-sectional			Longitudinal
Number of subjects	CTL: 406 PIVUS + 223 ADNI MCI: 325 ADNI AD: 176 ADNI	CTL Aβ+: 66 CTL Aβ-: 233	CTL Aβ-: 156 CTL Aβ+: 59 SCD Aβ+: 49 MCI Aβ+: 88	Visit 1 / Visit 2 / Visit 3 CTL: 137 / CTL: 137 / CTL: 24 SCD: 83 / SCD: 83 / SCD: 34 MCI: 74 / MCI: 74 / MCI: 24
MRI/MRS variables of interest	Intracranial volume 34 cortical volumes 17 subcortical volumes	68 cortical thickness measures	mI/Cr mI/NAA, NAA/Cr Cho/Cr	mI/Cr mI/NAA NAA/Cr Cho/Cr
Relevant demographic, pathologic and clinical variables	Age Gender Education	CSF Aβ42/Aβ40	CSF Aβ42, tau, p-tau APOE f-MRI Amyloid PET	CSF Aβ42 APOE MMSE
MRI/MRS sequence and processing	1.5 Tesla, T1 3D MPRAGE Freesurfer v. 5.1	3 Tesla, T1 3D MPRAGE Freesurfer v. 5.3	3 Tesla, PRESS sequence TE=30 ms, TR=2000 ms LCmodel version 6.3	

Panel 1 | Overview of study design, subject cohorts and methodology.

Intracranial volume in Freesurfer

The image most commonly used in the Freesurfer pipeline is a T1-weighted image, due the high contrast between GM and WM. However, CSF and bone are both dark in a T1 image, making it difficult to precisely identify the volume inside the skull. Total ICV was found to correlate well with the determinant of the transformation matrix (atlas scaling factor) used to register the image to an atlas (Buckner et al., 2004). Therefore, instead of performing segmentation, Freesurfer uses this relationship to estimate the ICV as follows,

$$eTIV = \frac{ICV_{atlas}}{atlas\ scaling\ factor} \qquad (3.1)$$

where eTIV stands for Estimated Total Intracranial Volume and is the nomenclature used by Freesurfer. For consistency, the term ICV is used throughout this thesis. The ICV estimated by Freesurfer is in good agreement with reference "gold-standard" segmentation (Nordenskjöld et al., 2013) and remains the preferred method for ICV estimation in large-scale imaging studies.

3.3.2 MRS acquisition and analysis (Studies III-IV)

Single-voxel MRS was performed on a Siemens TrioTim scanner at 3 Tesla, using the PRESS (Point RESolved Spectroscopy) sequence, at an echo time (TE) of 30 ms and repetition time (TR) of 2000 ms.

The 2×2×2cm^3 voxel was placed midsagittally in the posterior cingulate/precuneus (Figure 4). The posterior cingulate/precuneus region is highly involved throughout the course of AD pathology (Braak and Braak, 1991; Lehmann et al., 2010; Minoshima et al., 1997) and has recently been demonstrated as the earliest site for amyloid accumulation (Palmqvist et al., 2017). This region has also been used previously in large-scale MRS studies (Gomar et al., 2013; Nedelska et al., 2017) and was recommended for MRS studies in AD by the MRS consensus group (Öz et al., 2014).

In MRS, the obtained spectrum can be seen as a superposition of individual signals from separate compounds (Figure 2). The contributions from individual metabolites are isolated by fitting a linear combination of model spectra to the acquired *in vivo* MRS spectrum. Throughout this thesis, spectral analyses were performed using the LCModel software (Provencher, 1993, 2001). Model spectra (the basis set) are simulated using information about the sequence, field strength and acquisition parameters and subsequently adjusted to precisely fit the obtained MRS spectrum.

All MRS spectra were visually inspected for quality and artefacts. Only spectra with FWHM (full width at half maximum) ≤ 11 Hz were considered. Standard error estimates generated by the LCModel (Cramér-Rao lower bounds, %SD) were used as reliability indicators for metabolite concentrations. The value of %SD < 20% is often used as a limit for acceptable reliability. In this thesis, %SD was at or below 7% for all metabolites of interest.

3.3.3 Data analysis

Volume normalization

There are different ways to account for the effect of the total ICV in volumetric studies. The need for normalization arises from the fact that regional brain volumes are positively associated with the ICV and this association is assumed to be approximately linear. This section will present an overview of the most established methods of ICV adjustment.

The proportion approach calculates the ratio between the volume of interest and the total ICV, producing values between 0 and 1.

$$Volume_{adj} = \frac{Volume_{raw}}{ICV} \qquad (3.2)$$

This method is easy to use and can be applied to data from an individual subject without being influenced by the study cohort. It is important to keep in mind that this approach is appropriate only when the percentage of the cranial cavity occupied by a certain region is of particular interest. Bluntly comparing proportional volumes between two groups with different ICV will produce biased results.

The residual approach estimates the linear association between regional volumes ($Volume_{raw}$) and *ICV* to predict the ICV-adjusted volumes ($Volume_{adj}$). It may be described as:

$$Volume_{adj\,i} = Volume_{raw\,i} - \beta(ICV_i - ICV_{mean}) \qquad (3.3)$$

where β is the slope of the regression line between the *ICV* and the volume of interest. The adjusted volumes are obtained from the residuals of this linear regression and are therefore statistically uncorrelated with the *ICV*:

$$Volume_{adj\,i} = Volume_{raw\,i} - \beta(ICV_i - ICV_{mean})$$

$$Volume_{adj\,i} = \underbrace{Volume_{raw\,i} - \beta \cdot ICV_i}_{\text{Volume}_i - \text{E(Volume)} = \text{residuals}_i} + \underbrace{\beta \cdot ICV_{mean}}_{\text{mean volume}} \qquad (3.4)$$

$$Volume_{adj\,i} = Volume_{mean} + \varepsilon_i \qquad (3.5)$$

where ε is the residual term, i.e. the random variation not explained by the linear association.

This approach requires a reliable cohort from which the linear association is to be estimated. Also, in a group comparison setting, the choice has to be made whether the β from one or both groups should be used to estimate the *Volume-ICV* association. A common approach when comparing patients to controls is to use the β from the control group only to adjust both groups. The assumption being that the control group β represents the "normal" relationship between *Volume* and *ICV*.

The covariate approach is one of the most common methods for accounting for the ICV. As the name suggests, the ICV is included as a covariate in a linear regression model. For example,

in a volumetric study investigating gender differences, a linear regression model may take the following form:

$$Volume = \beta_0 + \beta_1 Age + \beta_2 Gender + \beta_3 ICV + \varepsilon \quad (3.6)$$

Where $\beta_0, \beta_1 \ldots \beta_n$ are regression coefficients - parameters which estimate the extent of variance in *Volume* associated with the variables *Age*, *Gender* or *ICV*. This model works well when the association between *Volume* and *ICV* is the same for both genders, i.e. when their slopes are parallel. Otherwise an interaction term is included in the model.

Analysis of brain connectivity

Cortical thickness measurements generated by the FreeSurfer pipeline using the Desikan atlas were used to define the network nodes (Desikan et al., 2006). The 68 thickness values (34 for each hemisphere) were adjusted for the effects of age and gender using linear regression. The graph edges were defined as the Pearson correlations between every pair of regions. They were computed and recorded in a 68×68 connectivity matrix. These matrices were binarized, such that the correlations above a certain value are set to one and those below the threshold are set to zero. A range of threshold densities (S_{min}=30% to S_{max}=50%, sampled in steps of 0.5%) was applied to each group's respective correlation matrix, ensuring that the two groups had the same number of edges. Negative correlations were excluded from the analyses. The graph properties in Study II were selected to cover the major aspects of network topology: integration, segregation and centrality.

Global efficiency is a measure of network integration, assessing how well information is exchanged across the system. The *global efficiency* measure is based on the inverse path length between nodes (Latora and Marchiori, 2001).

Clustering is the most frequently reported segregation measure, reflecting the extent to which the nodes surrounding a certain node are also neighbours with each other (Watts and Strogatz, 1998). *Transitivity* is similar to *clustering*. The *clustering* coefficient is normalized at a nodal level, whereas the *transitivity* is normalized at a network level (Newman, 2003). *Transitivity* may be a more appropriate measure to use in networks with poorly connected nodes.

Modularity reflects the presence of nodal groups or communities within the network. Networks with high modularity have a structure characterized by a high number of within-module connections and a low number of between-module connections (Newman, 2006).

The presence of *hubs* was also assessed. Hubs are nodes in a network characterized by having a large fraction of shortest paths run through them. Network hubs are network regions of extra importance for information transmission (Rubinov and Sporns, 2010).

Group comparisons were performed using non-parametric permutation testing with 1000 replications (Bassett et al., 2008; He et al., 2008). Network measures and group differences were computed in BRAPH – a graph theory software for the analysis of brain connectivity (Mijalkov et al., 2017), freely available at www.braph.org.

Mixed effect models

Linear mixed effect (LME) models are a powerful tool with a broad range of applications. LME models have many advantages over conventional data analysis methods, particularly when modeling longitudinal or repeated measures data. The main feature of LME models is that they incorporate fixed and random effects. Usually, if all possible levels of a factor are present in the experiment (e.g. gender, APOE genotype) they are modelled as fixed effects. If the experimental setup only contains a random sample of possible levels (e.g. subjects) the effect is modelled as random. In study IV, models with subject-specific intercepts and fixed slopes were constructed.

If some variable y_{ij} is measured in a group of individuals at several time points, the simplest form to model y_{ij} is:

$$y_{ij} = \beta + e_{ij} \qquad (3.7)$$

where

y_{ij} is the outcome measure for subject *i* at time point *j*,
β is the mean value of the outcome variable for all subjects at all time points,
e_{ij} is the error, assumed to be independently distributed $e_{ij} \sim N(0, \sigma^2)$.

To incorporate the subject-specific effect, the model can be expressed as

$$y_{ij} = \beta_i + e_{ij} \qquad (3.8)$$

where β_i is now the mean value of the outcome variable for subject *i*.

Model (3.8) only models a specific subset of subjects in the experiment and does not make inference on the population. A random-effect model (3.9), models the individual subject effect as $\beta + b_i$, rather than a constant value. Here, the β is the mean value across subjects and b_i is a random variable representing a deviation from a population mean and following the distribution $b_i \sim N(0, \sigma_b^2)$.

The mixed effect model takes the form:

$$y_{ij} = \beta + b_i + e_{ij} \qquad (3.9)$$

where

β is the mean value of the outcome variable across the sampled population,
b_i is the deviation from the population mean of the *i*th subject, $b_i \sim N(0, \sigma_b^2)$.
e_{ij} is the error, representing the deviation of the outcome value for subject *i* at time *j* from the mean value for subject *i*, where $e_{ij} \sim N(0, \sigma^2)$

Observations made on the same individual share the same random effect b_i and their covariance is accounted for through σ_b^2.

4 STUDY SUMMARY AND MAIN FINDINGS

This section describes the most important findings of the studies included in this thesis. Study I and Study II are discussed separately. Studies III-IV are assessed together.

4.1 STUDY I: INTRACRANIAL VOLUME ADJUSTMENT IN VOLUMETRIC MRI

Inter-individual differences in ICV may confound the results of volumetric MRI studies. There is little agreement regarding the appropriate method for ICV normalization of regional brain volumes in imaging studies of neurodegeneration. Study I highlights the implications of working with 1) unadjusted volumes 2) volume-to-ICV fractions (proportional approach) and 3) volumes from which the ICV effect has been regressed out (residual approach). Freesurfer-generated cortical and subcortical volumes from the PIVUS cohort (N=406) and the ADNI cohort (N=724) were examined (See Table 1 and Table 2 for demographics)

In the PIVUS cohort (healthy elderly aged 75) all unadjusted regional structures correlated positively with the ICV. Expressed as fractions of the ICV, the correlation direction was reversed for all gray matter structures. Third ventricle and lateral ventricles maintained a positive association with ICV even after division. The residual method, by definition, created residuals that were statistically uncorrelated with the ICV (Figure 7 and Figure 8). When the adjustment strategies were applied to the CTL, MCI and AD groups of the ADNI cohort, the results were qualitatively similar to the PIVUS findings. The positive association between regional volumes and ICV was reversed for all region-to-ICV gray matter fractions, but not for the ventricular fractions.

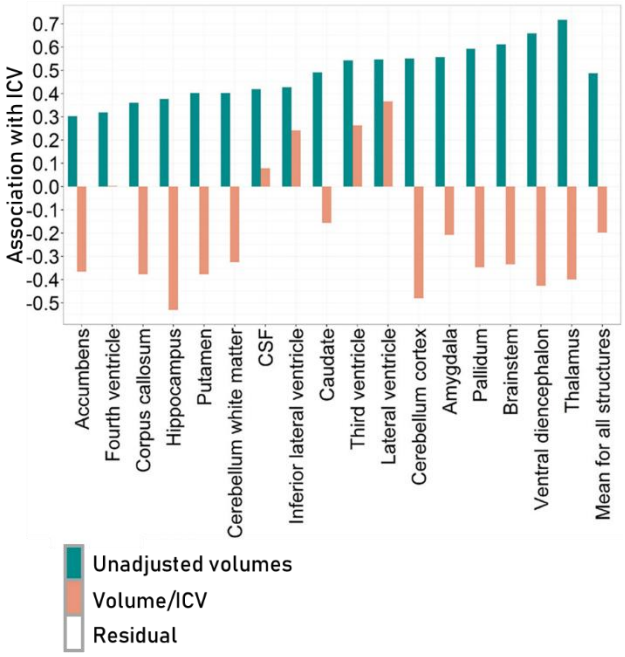

Figure 7 | Correlation patterns for individual regional subcortical volumes in the PIVUS cohort using different ICV adjustment approaches.

Further, we investigated the role of the different normalization approaches in a group comparison setting. Selected results of the gender comparisons in the PIVUS cohort are presented below.

Subcortical volumes were significantly greater in males than females ($p<0.05$) (although cerebellum WM and hippocampus did not survive the Bonferroni correction for multiple comparisons). When expressed as fractions of ICV, the majority of GM structures appeared to be significantly greater in women ($p < 0.05$), except for the lateral and third ventricles which remained larger for men even after dividing with ICV. The residual approach led to the removal of any significant volume differences between females and males.

In brief, the results of Study I indicate that:

1) The proportion approach does not completely remove the effect of ICV from a regional brain volume.
2) Although larger brains contain larger structures, they also contain proportionally more CSF than smaller brains.
3) Regressing out the ICV from volumetric measures removes all detectable differences in regional volumes between men and women.

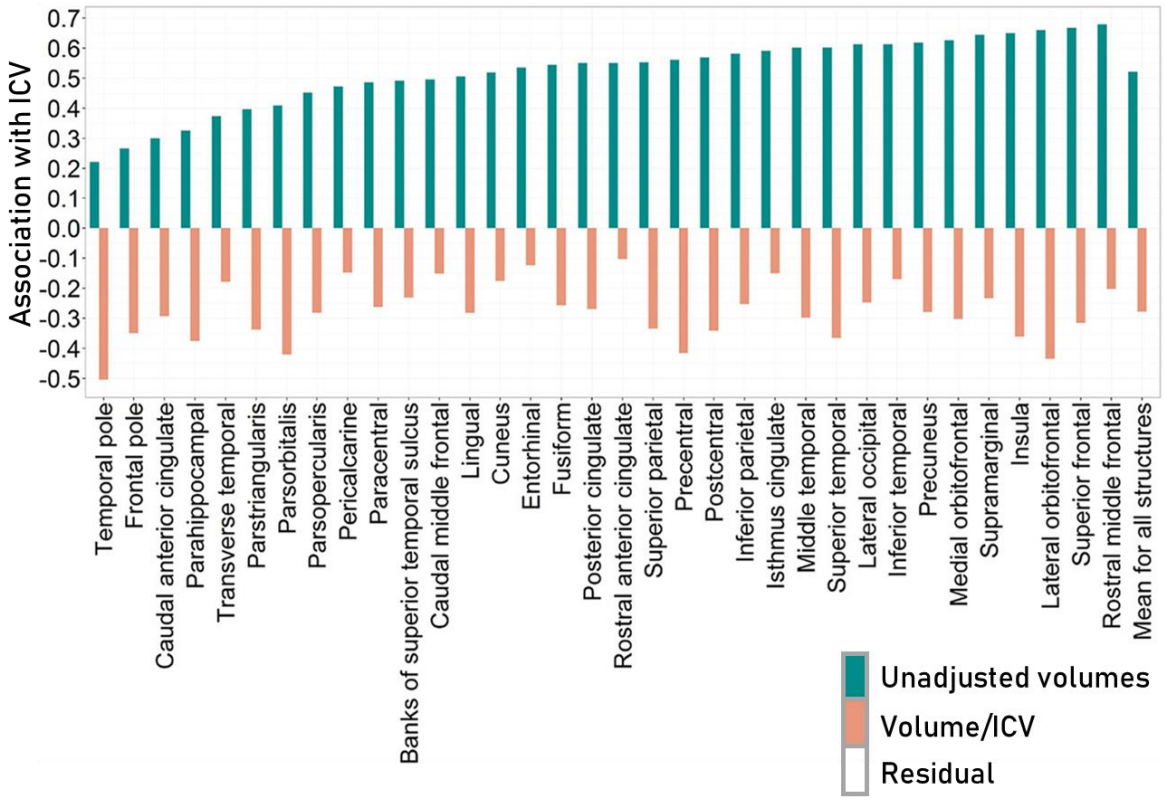

Figure 8 | Correlation patterns for individual regional subcortical volumes in the PIVUS cohort using different ICV adjustment approaches.

4.2 STUDY II: STRUCTURAL NETWORK ORGANIZATION

Global and local network changes were assessed in a cohort of cognitively healthy individuals (N=299), the CTL subset of the BioFINDER study. Structural networks were constructed based on 68 Freesurfer-generated cortical thickness values specified by the Desikan atlas. Group demographics can be found in Table 3, where participants with abnormal values of CSF Aβ42/Aβ40 (≤ 0.1) were considered amyloid-positive.

The CSF Aβ+ group was significantly older and had a higher percentage of ε4 carriers than the CSF Aβ- group. There were no differences in the average or regional cortical thickness between the groups at p=0.05.

Figure 9 represents the analysis flow. Weighted correlation matrices were constructed, binarized at a set density threshold, allowing for calculation of the network property of interest

for both groups. Group differences were obtained for each density by non-parametric permutation testing.

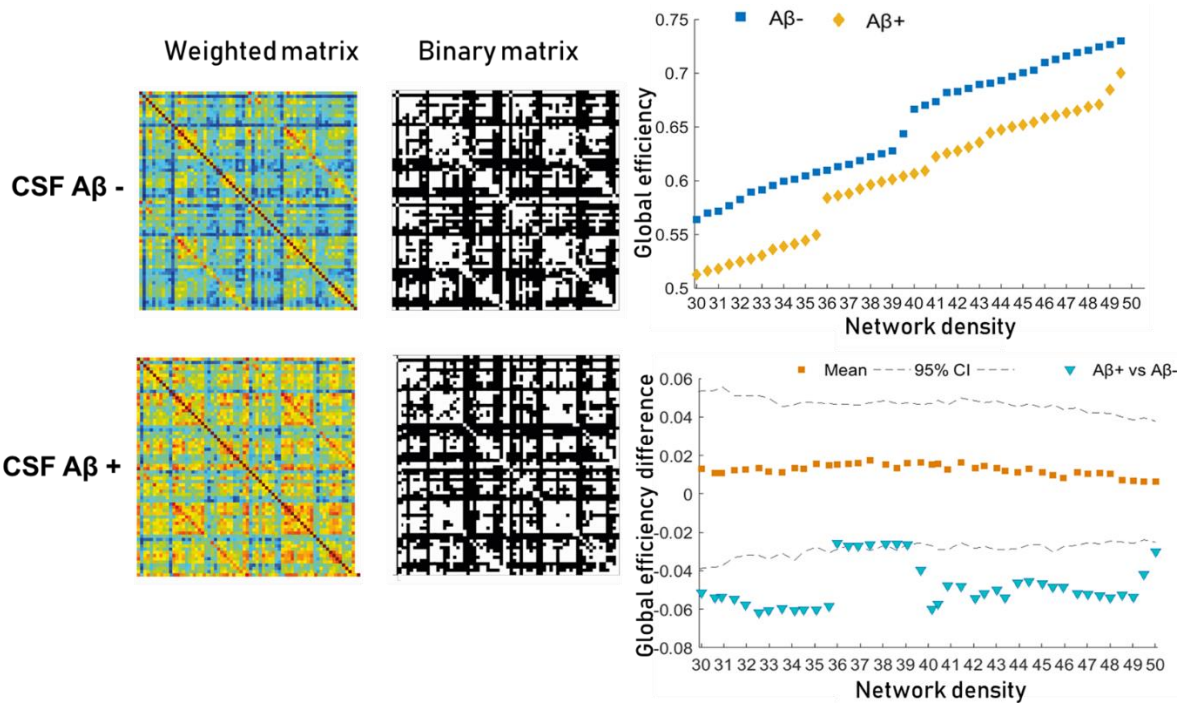

Figure 9 | Graph theory analysis flow. For each subject group weighted correlation matrices were computed and binarized. The network property of interest was calculated at all density values. Group differences were investigated for each density by non-parametric permutation testing.

CSF Aβ- and CSF Aβ+ groups displayed significant differences in global network properties at the density range 30%-50%. The CSF Aβ+ group had reduced global efficiency and reduced modularity across most densities after permutation testing. Transitivity and clustering tended to be elevated in the CSF Aβ+ group, although the results were less stable. When APOE ε4 carriers were compared to non-carriers, no significant differences were detected.

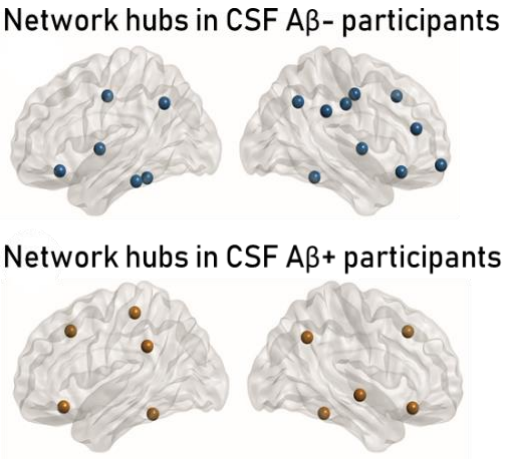

Figure 10 | Loss of hubs in the Aβ+ group

Furthermore, we detected a loss of network hubs in the CSF Aβ+ group. Network hubs are nodes that have a large number of shortest paths between pairs of nodes passing through them. In this study, hubs were defined as regions with betweenness centrality greater than 1.5 standard deviation from the group average. The most noteworthy hubs lost in the Aβ+ group were the precuneus and the right posterior cingulate – regions belonging to the DMN and therefore of relevance in the earliest AD stages.

In brief, the results of Study II suggest that:

1) Gray matter network changes in asymptomatic Aβ-positive elderly precede detectable cortical thinning.
2) Evidence of amyloid pathology is linked to reduced global efficiency, modularity and loss of hubs.

4.3 STUDIES III-IV: MAGNETIC RESONANCE SPECTROSCOPY IN PRECLINICAL ALZHEIMER'S DISEASE

In Study III, high quality MRS data was obtained from 352 elderly individuals and analyzed in conjunction with known dynamic AD biomarkers CSF Aβ and tau levels, amyloid PET, resting state fMRI and the genetic risk-factor *APOE*. Four study groups were chosen to mimic the hypothetical continuum of pre-dementia AD. The groups were: 1) cognitively healthy elderly with normal CSF Aβ42 (CTL Aβ-), 2) cognitively healthy elderly with abnormal CSF Aβ42 (CTL Aβ+), individuals with SCD and abnormal CSF Aβ42 (SCD Aβ+) and individuals with MCI and abnormal CSF Aβ42 (MCI Aβ+).

This study highlights the very early involvement of brain myo-inositol in AD progression. Elevated levels of mI/Cr were detected in the CTL Aβ+ group compared to the CTL Aβ- group ($p<0.05$). Furthermore, in the entire control group, an elevation in mI/Cr (and not a decrease in NAA/Cr) was associated with a decline in Aβ42 concentration in the CSF ($\hat{\beta} = -0.21$, $p = 0.002$) and a higher Aβ load on PET imaging ($\hat{\beta} = 0.32$, $p<0.001$). Reduced NAA/Cr was associated with an increase in CSF total tau in the MCI Aβ+ group ($\hat{\beta} = -0.24$, $p = 0.02$). Both measures reflect the extent of neuronal injury and are therefore expected to change at the MCI stage.

Another noteworthy finding of Study III was in participants with no cognitive decline or biomarker abnormalities. In the CTL Aβ42- group, mI/Cr levels were higher in APOE ε4 carriers compared to the non-carriers ($p<0.001$).

The main results of Study III suggest that:

1) Brain mI levels are changed already at asymtpomatic stages of AD.
2) APOE ε4 carriers with normal biomarker levels display elevated brain mI.

Study IV expands upon the results of Study III, by investigating for the first time the link between the changes in MRS metabolites over time and amyloid pathology. In Study IV, serial MRS data from 294 participants (CTL, SCD and MCI) was collected over a period of up to four years, resulting in 670 individual high-quality spectra. Furthermore, we took a particular interest in the NAA/mI ratio, due to the emerging evidence of the relevance of this measure in AD (Nedelska et al., 2017; Schreiner et al., 2018).

Table 6 | Visit time and number of acquired spectra in Study IV

	Time from baseline Years, mean (SD)	All subjects	CTL	SCD	MCI
Visit 1	0	294	137	83	74
Visit 2	2.28 (0.38)	294	137	83	74
Visit 3	4.10 (0.19)	82	24	34	24

As opposed to Study III where we prioritized including individuals with abnormal CSF Aβ42 levels, in Study IV, all subjects with multiple MRS were included irrespective of amyloid pathology evidence (Table 5).

Using linear mixed effect models to estimate the rates of change in the ratios mI/Cr and NAA/mI, we demonstrate that the trajectory of longitudinal changes in mI differs significantly depending on the presence of underlying amyloid pathology. An example of a mixed model used in Study IV is presented in (Table 7). This model assesses whether baseline Aβ status affects the rate of change in mI/Cr and NAA/mI, accounting for age, sex and APOE ε4 carriership. The primary predictor of interest is the interaction between Aβ status and visit number.

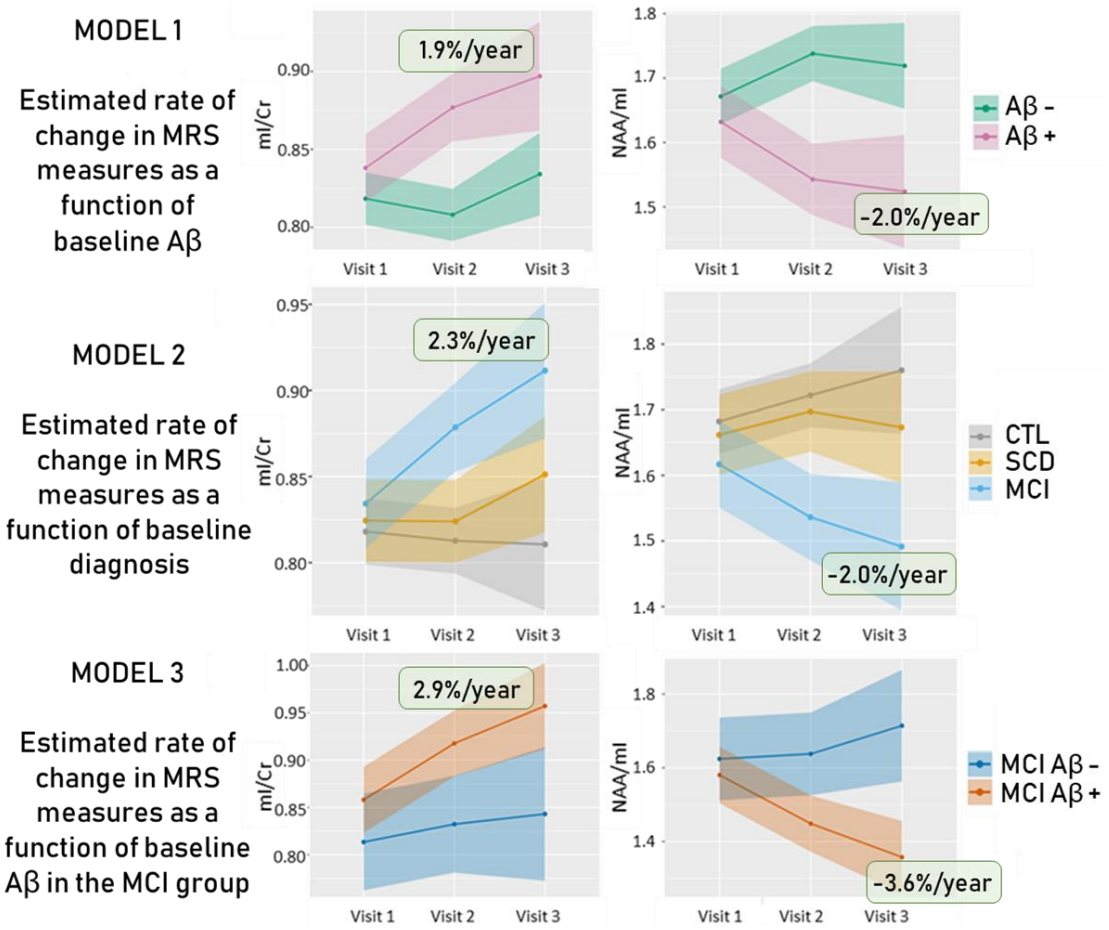

Figure 11 | Estimated rates of change of MRS measures mI/Cr and NAA/mI in different biomarker and diagnostic groups

In Aβ+ individuals mI/Cr increased at an estimated yearly rate of 1.9%, whereas in the Aβ- group the rate of change was negligible at 0.3%/year. NAA/mI declined at a rate of 2.0%/year in the Aβ+ group. Additional models were built to: 1) explore the role of diagnosis-by-visit interaction and 2) investigate whether the Aβ-by-visit interaction is a relevant predictor when only the MCI group is considered. Figure 11 presents the estimated trajectories of metabolite measures mI/Cr and NAA/mI as well as the annualized rates of change in various diagnostic and biomarker groups. Perhaps unsurprisingly, the greatest MRS variation was detected in the Aβ+ MCI group, where NAA/mI decreased at a rate of -3.6% per year.

Table 7 | Example of a mixed model used to estimate the rate of change of mI/Cr and NAA/mI

	Outcome measure: mI/Cr		Outcome measure: NAA/mI	
Fixed effects	Estimate (SE)	P value	Estimate (SE)	P value
Intercept	0.10 (0.08)	< 0.001	1.43 (0.20)	<0.001
Aβ	0.02 (0.02)	0.18	-0.04 (0.04)	0.29
Visit 2	-0.01 (0.01)	0.21	0.07 (0.37)	0.001
Visit 3	0.02 (0.01)	0.24	0.05 (0.02)	0.15
Age	-0.00 (0.00)	0.09	0.00 (0.00)	0.20
APOE	0.02 (0.01)	0.16	-0.07 (0.03)	0.045
Gender	-0.03 (0.01)	<0.01	-0.07 (0.33)	0.05
Aβ × Visit 2	0.05 (0.01)	<0.001	-0.16 (0.03)	<0.001
Aβ × Visit 3	0.04 (0.02)	<0.05	-0.16 (0.05)	<0.01

The finding linking APOE ε4 carriership to higher mI concentrations in Aβ-negative individuals (Study III) did not uphold in the longitudinal follow-up. We found no evidence that ε4 carriers accumulate mI at a faster rate than ε4 non-carriers.

Since longitudinal MMSE data was available for Study IV participants, we explored whether baseline levels of NAA/mI were associated with the rate of future cognitive decline. We found that in the Aβ+ group, the trajectory of MMSE decline was significantly different for those with low baseline NAA/mI compared to those with high baseline NAA/mI ratio. Aβ+ individuals with baseline NAA/mI<1.5 lost a total of 6.3 MMSE points, whereas Aβ+ individuals with baseline NAA/mI≥1.5 lost a total of 2.2 MMSE points in four years. In the Aβ- group the MMSE showed negligible variability during the four year time period.

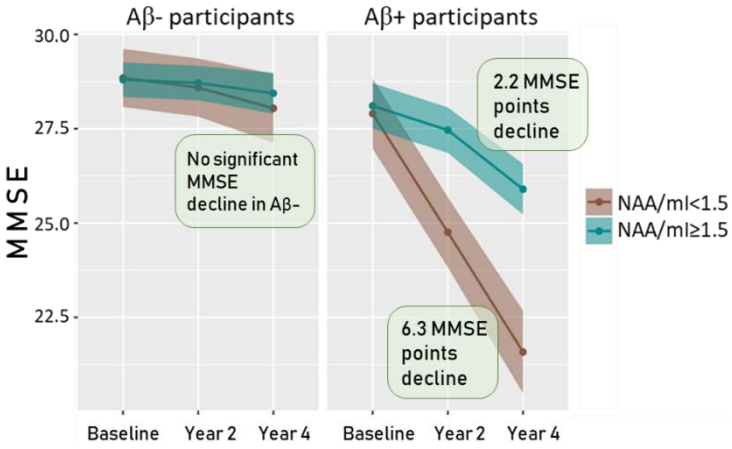

Figure 12 | Estimated rates of change of MRS measures mI/Cr and NAA/mI in different biomarker and diagnostic groups.

The main results of Study IV indicate that:

1) Longitudinal changes in mI are largely governed by the presence of amyloid pathology.
2) Stratifying Aβ+ individuals based on baseline NAA/mI values may reveal subgroups with markedly different rates of cognitive decline over time.

5 DISCUSSION

5.1 WHAT DOES IT MEAN TO BE "AMYLOID-POSITIVE"?

A substantial part of this thesis deals with cognitively healthy individuals with evidence of amyloid pathology, i.e. a population believed to be at higher risk for AD. Although evidence of brain amyloid accumulation is the earliest AD hallmark, it is still unclear exactly how abnormal levels of Aβ are related to brain atrophy and cognitive decline. About 20-30% of older people show evidence of elevated brain amyloid (Aizenstein et al., 2008; Jansen et al., 2015; Mattsson et al., 2015). The question is, are all these people heading towards an AD diagnosis? What does it mean to be amyloid-positive? First of all, it is important to recognize that harbouring amyloid might be a natural process related to ageing. It has been found that 12% of healthy 60 year-olds are amyloid-positive, among 70 year-olds it is 30%, and among cognitively normal 80 year-olds approximately half show evidence of Aβ accumulation (Rowe and Villemagne, 2011). Villemagne and colleagues have also shown that for someone who has just reached the amyloid-positive threshold, the signs of mild cognitive impairment are expected to appear about 14 years later, and a dementia diagnosis is decades away (Villemagne et al., 2013). This means that cerebral amyloid accumulation in the very old should perhaps not be seen as alarming, since the "silent" phase of preclinical pathology might be so long that it may not be relevant.

Nevertheless, the involvement of amyloid in processes detrimental to the brain cannot be refuted. There is substantial evidence from longitudinal studies of increased brain atrophy rates in cognitively normal amyloid-positive elderly (Andrews et al., 2013; Chételat et al., 2011; Schott, J. et al., 2010; Villemagne et al., 2013). In functional MR studies, Aβ accumulation has consistently been linked to alterations within the DMN (Mormino et al., 2011; Sheline et al., 2010), which seems sensible, since the DMN and the regions of amyloid deposition have a largely overlapping topography (Buckner et al., 2005). Although the relationship between amyloid plaques and the severity of cognitive decline in AD is not straightforward, longitudinal studies have demonstrated that in cognitively normal elderly, amyloid-positivity is associated with steeper cognitive decline (Fagan et al., 2007; Resnick et al., 2010). A recent study assessing cognition in middle-aged adults (age 40 to 59), demonstrated a detectable decline in vocabulary within the amyloid-positive group (Farrell et al., 2017).

The link between Aβ pathology and the harmful structural, functional and cognitive processes, together with the increasing availability of CSF and amyloid PET data, have motivated many researchers to focus their attention on the group of cognitively normal Aβ-positive people, taking this group to represent the very first stage of the AD continuum, as per the definition of preclinical AD (Sperling et al., 2011). In studies II-IV this framework was employed to explore whether network organization, or MRS metabolites are altered in amyloid-positive non-demented elderly. Indeed, older Aβ-positive asymptomatic individuals exhibited changed global and local network parameters. Among others, they presented with significantly lower global efficiency, higher clustering, a loss of hubs and a reorganization of network modules, demonstrating that brain networks are sensitive to underlying amyloid pathology. Brain

metabolites evaluated with MRS, specifically measures containing myo-inositol measured in the posterior cingulate/precuneus region, also showed substantial cross-sectional and longitudinal changes in asymptomatic at-risk individuals. Neither graph theory (study II) nor MRS (studies III-IV) belong to the realm of established AD biomarkers, and relatively little is known about their interplay with other markers of pathology. Exploring these more "unconventional" biomarkers of AD, and demonstrating their sensitivity to ongoing brain amyloidosis, can be considered one of the connecting themes of this thesis.

5.2 BRAIN ARCHITECTURE

Brain structure and function are determined by a constellation of genetic and environmental factors, age and pathology. Understanding the changes taking place in the brain during normal ageing is essential for identifying and characterizing disease-related phenomena. Several conceptual and methodological factors have moved structural MRI studies towards working predominantly with multiple volumetric and cortical thickness measures rather than with a priori selected brain regions. Such, in the field of AD, seminal studies regarding the early atrophy of the hippocampus and the entorhinal cortex (Fox et al., 1996; Scheltens et al., 1992) are being complemented by research on distinct patterns of brain atrophy and the probable existence of distinct disease subtypes (Ferreira et al., 2017; Poulakis et al., 2018). This shift towards multiple brain region analysis has been made possible by the availability of sophisticated computerized segmentation techniques.

Exploring structural covariance is one of the two main themes of this thesis. Notably, in Studies I and II, this phenomenon is addressed in conceptually distinct manners. In Study I, where the interrelationship of regional brain volumes and the total ICV is assessed, the existence of structural co-variance is largely interpreted as an obstacle, something that confounds the interpretation of the results, or as Barnes and colleagues refer to it, "a necessary nuisance" (Barnes et al., 2010). On the other hand, in Study II, the phenomenon of structural co-variance is made the most of - it is the foundation for graph construction subsequent detection of otherwise indiscernible patterns.

Evidence from neuroimaging studies reveals that the ageing brain decreases in total volume (Barnes et al., 2010; Courchesne et al., 2000; Scahill et al., 2003), gray matter volume (Courchesne et al., 2000; Good et al., 2001) and cortical thickness (Sowell et al., 2007). Longitudinal studies estimate annual brain volume decline to be approximately 0.5% per year (Fjell et al., 2009). The independent effect of age has been the focus of many neuroimaging studies of neurodegeneration since age variability often interferes with evaluating the extent of "true" pathology. Another common confounder in cross-sectional volumetric studies is the ICV – an estimate of the maximal brain volume. Larger brains tend to contain larger structures, so for example, when two people of the same age and gender, yet substantially different head sizes have similar-sized hippocampi, a disease-specific atrophic process might already be underway in the person with the larger ICV.

In Study I we worked with MRI images from a unique cohort of over 400 healthy individuals all scanned at age 75 using a single MR system. Thus, in this dataset, age - a major source of between-subject variability – was eliminated by design, creating an ideal setup for investigating the implications of ICV adjustment. Men generally have larger cerebra than women (Blatter et al., 1995; Coffey et al., 1998; Gur et al., 1991; Raz et al., 2004); in line with this evidence we too report that uncorrected regional volumes are greater in males than females. Assessing gender dimorphism *per se* was not the main objective of the study, but nevertheless provided an illustrative example of a group-comparison setting where ICV may obscure or exaggerate true differences. We found that regressing out the effect of ICV from the data removed any detectable structural differences between males and females. The more interesting finding emerged from looking at region-to-ICV fractions: GM structures were greater in women, whereas ventricular structures were greater in men. If age-related atrophic changes have progressed further in men than women by the age of 75, it implies that volumetric decline commences at an earlier stage and/or progresses at a faster rate in men. The observation of faster age-related volumetric decline, and ventricular expansion is supported by several studies (Barnes et al., 2010; Blatter et al., 1995; Coffey et al., 1998; Gur et al., 1991; Raz et al., 2004). Study I was designed to describe the relationship between regional volumes and ICV, and to bring to light how this relationship changes depending on the choice of ICV normalization strategy. Several studies discuss the statistical reliability of the various ICV-adjustment strategies, pointing out the relative sensitivity to error of the proportional method (Arndt et al., 1991; Sanfilipo et al., 2004). However, experience tells us that the choice of how to adjust for ICV is more likely to be influenced by a particular research question or the conventions existing within the research field. An idea seldom expressed in the context of brain volumetric studies, is whether it may in some cases be useful to report both adjusted and unadjusted volumes, since the absolute volume of a structure and its size relative to the total brain volume essentially provide complimentary information. Of note, when it comes to cortical thickness regions, ICV adjustment is probably not required (Barnes et al., 2010; Westman et al., 2013).

Another way of working with gray matter morphological measures is by looking at them from a network perspective. In network modeling, the brain is represented as a graph: a set of nodes interconnected by edges. Within the domain of brain topology, graphs can be built using data from most of the major imaging modalities. In diffusion tensor imaging, edges of a graph are the probable axonal connections between pairs of gray matter regions. In f-MRI, an edge represents a functional connection – two regions that demonstrate similar dynamics of activation over time. In Study II, brain networks were constructed from structural MRI, and the edges defined by structural co-variance between pairs of gray matter regions. We aimed to investigate whether individuals at risk for AD display detectable alterations in brain connectivity metrics based on cortical thickness data. Cortical thickness measures were used since they are known to be sensitive to the very early changes of the pre-dementia AD pathology (Dickerson et al., 2009). Longitudinal studies have shown that cortical thinning predicts steeper cognitive decline later in life (Dickerson and Wolk, 2012; Pacheco et al., 2015) and conversion to AD dementia (Bakkour et al., 2009). The results of our study suggest that

structural connectivity changes occur before any cortical thinning can be detected. Individuals harbouring amyloid pathology did not display more cortical atrophy in any isolated region, yet they exhibited substantially different global and local network parameters. For example, global efficiency – the ability to rapidly integrate information was compromised in amyloid-positive individuals before the onset of symptoms or gray matter loss. Furthermore, we detected a loss of hubs in the at-risk group, in regions pertaining to the DMN. The involvement of the DMN in amyloid-related pathological processes has been demonstrated previously, particularly in a recent study by Palmqvist et al, where DMN regions (posterior cingulate and precuneus) were found to be the earliest sites of Aβ accumulation (Palmqvist et al., 2017).

An appealing aspect of network modeling is its ability to reduce a complex system to a set of concepts that, albeit abstract, are generalizable across a wide variety of fields. It is exciting to explore how patterns of brain topology compare to the complex systems of language, markets, sociology etc. At the same time there is a pressing need for a common language within the field of neuroscience – one which would address the interdependence between structure and function. The DMN is a good example of an abstract concept that is consistently detected by several imaging techniques and shows a striking overlap across structural and functional modalities (Greicius et al., 2009). The discovery and characterization of more of this type of ubiquitous phenomena may be one of the major prospective applications of graph theory.

5.3 ALZHEIMER'S DISEASE NEUROMETABOLIC SIGNATURE

The most consistent brain metabolic changes related to evolving AD pathology are an increase in mI and a decrease in NAA. Many studies have reported results for the composite ratio mI/NAA (or NAA/mI), demonstrating it to be more useful than MRS metabolites in several contexts. Such, mI/NAA is superior in discriminating between AD and controls (Kantarci et al., 2002; Martínez-Bisbal et al., 2004), predicting the onset of MCI (Kantarci et al., 2013) and accumulation of brain amyloid (Nedelska et al., 2017) in cognitively normal elderly individuals.

The results of this thesis also highlight the relevance of mI/NAA as a standalone measure and suggest that it should be reported in all MRS studies. In Study IV, where the longitudinal evolution of mI/NAA is presented alongside mI/Cr, it is evident that the difference in the MRS signature between the amyloid-positive and the amyloid-negative groups is amplified when the mI/NAA is used. As will be discussed below, the change observed in the composite ratio is likely to be driven by either mI or NAA depending on the stage of the disease.

We know from longitudinal studies that the mI elevation is an early event in AD pathology detectable already at asymptomatic pre-dementia stages, whereas the decrease in NAA occurs at a later time in the disease progression. There is no evidence of a reversal in mI levels at more advanced disease stages, and both mI and NAA are abnormal in established AD. The findings presented in this thesis locate the rise in mI at the very first stages of detectable pathology. Brain mI/Cr in cognitively normal controls with abnormal CSF Aβ42 is already changed and correlates with higher plaque deposition on amyloid PET imaging (Study III). This is in line

with evidence from quantitative histopathological assessment of the posterior cingulate region, which demonstrated a significant association between ante-mortem mI/Cr levels and post-mortem plaque density (both diffuse and cored) (Murray, M. E. et al., 2014). The authors found no relationship between Aβ plaque burden and NAA/Cr. Brain NAA was in turn associated with synaptic vesicle immunoreactivity and p-tau (Murray, M. E. et al., 2014). Also, in this thesis, no association between NAA and amyloid pathology has been established, but NAA/Cr was found to correlate with an increase in t-tau in amyloid-positive MCI (Study III). Taken together, this evidence suggests that mI and NAA are markers of different pathological processes – both hallmarks of AD.

Although we suggest that there exists an MRS metabolic "signal" of AD, picked up most reliably by the mI/NAA ratio, the practical usefulness of such a marker will depend on several factors. Evidence from murine models suggests that mI is able to detect the reduction in plaque deposition brought about by passive immunization targeting Aβ (Marjańska et al., 2014). However, although Aβ-modifying immunotherapies have shown great promise in animal models, their benefits in human studies are yet to be demonstrated (Wisniewski and Goñi, 2015). Since we assume that the association between mI and AD pathology is driven by Aβ, when mI is put forward as a potential marker of treatment efficacy, it is implied that the employed treatment strategy somehow affects brain Aβ load. Although trials explicitly aimed at removing plaques have not had a positive outcome (Salloway et al., 2014), it is probable that other types of disease-modifying therapies will indirectly influence the process of plaque aggregation or deposition (i.e. by targeting Aβ oligomers). So, conceptually mI is a relevant candidate for use in a clinical setting or a trial design. But what about the practical aspects? To be able to monitor treatment efficacy, the intra-individual variability in mI measurements must be minimal relative to the treatment effect. The test-retest reproducibility of single-voxel MRS in the posterior cingulate has been examined in a setup where healthy volunteers underwent weekly scans using clinical hardware at 3T, demonstrating minimal between-session coefficients of variance for the metabolites mI, NAA, Cho and Cr, as well as high reproducibility of the voxel placement (Terpstra et al., 2016). But when the time interval between two consecutive MRS exams is large enough for atrophic changes to take place, even a topographically consistent voxel placement may introduce intra-individual variability due to an altered voxel composition. However, the error introduced by partial volume effects is minimized when ratio-based quantification is performed. As for successful disease-modifying strategies and how they will manifest themselves in the spectroscopic signal, this remains to be elucidated. Schott and colleagues have previously discussed this matter in a longitudinal MRS study (Schott, J.M. et al., 2010). The authors speculate that if future treatment brings about a reverse of the AD-typical metabolite trajectories, then MRS will be a good response biomarker. However, if the treatments merely slow down the progression of metabolite abnormality, these effects may be confounded by within-subject measurement variance (Schott, J.M. et al., 2010). In any case, standardized protocols and clear guidelines for voxel placement in multi-center studies will aid in exploring the potential of MRS metabolites for monitoring treatment effects.

The type of brain cells giving rise to the total observed MRS signal cannot be determined easily. NAA is synthesized exclusively in the neuronal mitochondria, therefore is some consensus of NAA being a suitable marker of mitochondrial and neuronal integrity (Dautry et al., 2000; Moffett et al., 2007). However, the reductions in NAA can sometimes be reversed following a period of recovery or treatment (Maddock and Buonocore, 2012; Westman et al., 2007). The fact that NAA seems to pick up transient damage to neuronal function limits the usefulness of this metabolite as a standalone marker in AD.

When it comes to the biological mechanisms behind mI alterations in the early stages of AD, they are not fully understood. The mI signal has often been linked to glial activation and proposed as an *in vivo* marker or neuroinflammation, however whether mI is preferentially present in glial or neuronal cells is not clear. High mI concentrations have been detected in cultured astrocytes, but not in neurons (Brand et al, 1993), prompting the assertion of a glial source of this metabolite. However, this widely cited paper has a number of methodological limitations, which restrict its generalizability (discussed in full detail elsewhere (Maddock and Buonocore, 2012)). Briefly, cultured neurons and astrocytes used in the study were at widely distinct stages of development and neither were able to synthesize mI from glucose as is the case *in vivo*. However, when mI was added to the culture environment, it was taken up more readily by mature astrocytes than embryonic neurons. Fisher et al. reviewed several other studies addressing mI concentrations in cultured neuronal and/or glial cells, revealing that mI levels are comparable in both types of brain cells (Fisher et al., 2002). In the study assessing post-mortem neuropathologic correlates of the ante-mortem MRS signal. Murray et al. did not detect any significant association between mI and the microglial or astrocytic burden, once more putting into question the relationship between mI and gliosis in AD (Murray, M. E. et al., 2014).

One of the most important physiological functions of mI is that of an organic osmolyte (Kwon et al., 1992). Under osmotic stress the volume of the cell must be preserved so as not to disrupt important intracellular processes. In response to extracellular hypertonicity (such as hypernatremia) mI enters the cells (Lee et al., 1994) and effluxes the cell in hypotonic conditions (Videen et al., 1995). A recent study demonstrated that intracellular accumulation of mI in response to hypertonic stress increases the levels of polyphosphoinositide, thereby modulating neuronal activity via phosphoinositide-dependent ion channels (Dai et al., 2016). Dai and colleagues were the first to show that mI elevation due to osmoregulation affects electrical signaling of excitable cells (Dai et al., 2016). This suggests that the behavior of mI in pre-dementia AD may be reflecting the cells' attempt to endure homeostatic aberrations, and that mI may be linked to altered synaptic function independently of Aβ. More basic research of similar caliber to the Dai et al. study is needed to elucidate the mechanistic linkage between mI and the pathogenesis of AD. The lack of a clear understanding of the biological processes behind the MRS changes is one of the most apparent obstacles to broader use of this cost-efficient and non-invasive technique.

6 CONCLUDING REMARKS

The general aim of this work was to advance the characterization of structural and metabolic changes associated with incipient AD pathology. **Study I** addressed a common methodological issue of volumetric MRI studies related to inter-individual differences in ICV. This work demonstrates that the choice of ICV normalizations approach affects the interpretation of study results, highlighting the importance of a clear and transparent ICV adjustment strategy in volumetric MRI studies. **Study II** examined the organization of structural networks in cognitively healthy elderly with evidence of amyloid pathology, revealing aberrations in cerebral network topology in absence of detectable cortical thinning. **Study III** situated changes in the MRS profile within the context of existing clinical, pathologic and functional AD biomarkers, highlighting the involvement of brain mI at very early stages in the disease progression. **Study IV**, presented evidence that mI may have the ability to track AD-specific pathological processes. The results revealed that amyloid-positive individuals accumulate mI at a higher rate than people no evidence of amyloid pathology.

Throughout this thesis, early biomarker characterization has been addressed largely from the perspective of the research community, and therefore treated as something fundamentally positive. It should be recognized, however, that being able to assess a person's risk of developing an incurable disease, gives rise to obvious ethical challenges. Although detecting "amyloid-positivity" or APOE ε4 carriership among healthy elderly is important for clinical trials, disclosing such information in the clinic may be damaging to individuals and family members. Apart from the potential psychological risks involved, individuals may be subjected to unfair treatment in the workplace or the insurance market. This "genetic or biological" discrimination is one of the general risks associated with the emerging field of precision medicine (Hampel et al., 2016). More research is needed to guide the practical implementation of biomarker evidence of AD.

Another conceptual shift likely to advance medical research and aid the neuroimaging community in particular is related to the rapid advances in automated image recognition techniques. The total quantity of neuroimaging data is growing quickly, as is our capacity for information storage. Machine learning approaches, including deep learning are permeating the field of medical image analysis and becoming the method of choice for classification, object detection, segmentation etc. (Litjens et al., 2017). Today, these state-of-the-art methods are being applied mostly to high resolution imaging data. However, their potential is largely overlooked when it comes to the existing data of the scientific archives. A myriad of scans collected since the advent of medical imaging have been put on the shelf and deemed obsolete as new and improved imaging methods emerged. Incidentally, this "outdated" data may be particularly useful for research since it is likely to contain valuable follow-up information. In simple terms – new methods do not necessarily require new data to uncover novel information. Present day machine learning techniques can and should be applied to already existing imaging/spectroscopic data which has previously only been inspected visually.

As a final remark, I would like to acknowledge the immense importance of dedicated long-term care for dementia patients. In his 1985 book "The man who mistook his wife for a hat", Oliver Sacks recounts writing to A.R. Luria to seek his advice regarding a patient whose memory loss was beyond repair (Sacks, 1985). *"There are no prescriptions in a case like this. Do whatever your ingenuity and your heart suggest."* Luria writes. *"But a man doesn't consist of memory alone"*, he goes on, *"He has feeling, will, sensibilities, moral being – matters of which neuropsychology cannot speak. And it is here, beyond the realm of interpersonal psychology, that you may find ways to touch him, and change him. And the circumstances of your work especially allow this, for you work in a Home, which is like a little world, quite different from the clinics and institutions where I work."* Luria's message is clear - when science and medicine are rendered powerless, it is the empathy and the immense resourcefulness of those who care for patients day after day, that can make all the difference.

7 ACKNOWLEDGEMENTS

I would like to express my sincerest gratitude to:

Eric Westman, my main supervisor, for being a supportive and open-minded person, and for translating these traits into your approach to research and supervision. I appreciate that you value the balance between scientific freedom and responsibility, for this is the environment where confident and self-reliant researchers are formed. Thank you for being patient and for encouraging me to pursue my own ideas – it has been an immense pleasure working with you.

Lars-Olof Wahlund, my co-supervisor, for your kind support and encouragement; for sharing your unique expertise in dementia research and for always seeing the bigger picture. As the founder of our research group, your personal and scientific values set the tone for the positive attitude that characterizes the group today.

Oskar Hansson, my co-supervisor, for your sharp ideas and immense knowledge of the field. I'm grateful for all the expert advice you have given me and, of course, for introducing me to the amazing BioFINDER project.

Andrew Simmons, my co-supervisor, for your support, help and valuable guidance.

Katja Chernogubova, my mentor, for being a fantastic person, a true friend and a master chef.

Anette Eidehall for being the person that holds everything together and for always taking care of me. Thank you.

Nenad Bogdanovic, maestro, thank you for taking the time to share your wisdom and for putting up with my ignorance.

Aleksandra Lebedeva, for your insightful ideas, fascinating theories and your sense of humour. You are a treasure.

I'm grateful to all current and former members of the imaging group at the Division of Clinical Geriatrics. In particular I would like to thank:
Joana, for being fun, kind and very sharp, **Konstantinos**, for your invaluable help and enthusiasm; **Ale**, for our friendship and for being on the same wavelength; **Dani**, Dr. Ferreira, for always looking out for me; **Gustav**, for being a kindred spirit and an em-dash-enthusiast. **Camila**, for being an important part of my life – we have Clinical Geriatrics to thank for our friendship. **Una, Farshad, Soheil, Olof, Gabi, Carlos, Xiaozhen, Sebastian, Urban –** thank you for being great colleagues and contributing to a fun atmosphere at work. From the PET group: **Kostas, Elena, Laetitia, Antoine** and **Mariam** – I've really enjoyed working alongside you.

I would also like to thank co-workers outside the group, in particular: **Heela**, for being a brave and talented person, and an inspiration; **Irina Savitcheva**, for introducing me to the world of MR imaging; **Love**, for teaching me how to run the MR scanner; **Juraj** and **Emilia** for being easy-going and always very fun to talk to; **Märta,** for being lovely and fun; **Kristina Johnell,**

for being friendly and competent; **Maria Ankarcrona,** for always being helpful and **Mia Eriksdotter,** for doing an impressive job running the NVS department.

Jag vill även tacka min fina släkt och vänner:

Torbjörn och **Haidi Astlind**, för att ni alltid finns där för mig. Det finns knappt någon som känner mig bättre än ni, och definitivt ingen som tror på mig mer. **Rita** och **Linus**, för er vänskap och för våra barns vänskap. Vilken otrolig tur vi haft! **Familjen Jonsson-Malmberg** – tänk att jag lyckats ansluta mig till en sådan underbar klan!

Anders, tack för din kärlek och ditt stöd. **Du**, **Nina** och **Cora** är mitt favoritgäng och det bästa jag vet!

8 REFERENCES

Adalsteinsson, E., Sullivan, E.V., Kleinhans, N., Spielman, D.M., Pfefferbaum, A., 2000. Longitudinal decline of the neuronal marker N-acetyl aspartate in Alzheimer's disease. The Lancet 355(9216), 1696-1697.

Aizenstein, H., Nebes, R.D., Saxton, J.A., et al., 2008. Frequent amyloid deposition without significant cognitive impairment among the elderly. Archives of Neurology 65(11), 1509-1517.

Albert, M.S., DeKosky, S.T., Dickson, D., Dubois, B., Feldman, H.H., Fox, N.C., Gamst, A., Holtzman, D.M., Jagust, W.J., Petersen, R.C., Snyder, P.J., Carrillo, M.C., Thies, B., Phelps, C.H., 2011. The diagnosis of mild cognitive impairment due to Alzheimer's disease: recommendations from the National Institute on Aging-Alzheimer's Association workgroups on diagnostic guidelines for Alzheimer's disease. Alzheimers Dement 7(3), 270-279.

Andrews, K.A., Modat, M., Macdonald, K.E., Yeatman, T., Cardoso, M.J., Leung, K.K., Barnes, J., Villemagne, V.L., Rowe, C.C., Fox, N.C., Ourselin, S., Schott, J.M., the Australian Imaging, B., Lifestyle Flagship Study of, A., 2013. Atrophy Rates in Asymptomatic Amyloidosis: Implications for Alzheimer Prevention Trials. PLOS ONE 8(3), e58816.

Apostolova, L.G., Dutton, R.A., Dinov, I.D., et al., 2006. Conversion of mild cognitive impairment to alzheimer disease predicted by hippocampal atrophy maps. Archives of Neurology 63(5), 693-699.

Arndt, S., Cohen, G., Alliger, R.J., Swayze Ii, V.W., Andreasen, N.C., 1991. Problems with ratio and proportion measures of imaged cerebral structures. Psychiatry Research: Neuroimaging 40(1), 79-89.

Arriagada, P.V., Growdon, J.H., Hedley-Whyte, E.T., Hyman, B.T., 1992. Neurofibrillary tangles but not senile plaques parallel duration and severity of Alzheimer's disease. Neurology 42(3 Pt 1), 631-639.

Bakkour, A., Morris, J.C., Dickerson, B.C., 2009. The cortical signature of prodromal AD: Regional thinning predicts mild AD dementia. Neurology 72(12), 1048-1055.

Barnes, J., Ridgway, G.R., Bartlett, J., Henley, S.M.D., Lehmann, M., Hobbs, N., Clarkson, M.J., MacManus, D.G., Ourselin, S., Fox, N.C., 2010. Head size, age and gender adjustment in MRI studies: a necessary nuisance? NeuroImage 53(4), 1244-1255.

Bassett, D.S., Bullmore, E., Verchinski, B.A., Mattay, V.S., Weinberger, D.R., Meyer-Lindenberg, A., 2008. Hierarchical Organization of Human Cortical Networks in Health and Schizophrenia. The Journal of neuroscience : the official journal of the Society for Neuroscience 28(37), 9239-9248.

Bateman, R.J., Xiong, C., Benzinger, T.L.S., Fagan, A.M., Goate, A., Fox, N.C., Marcus, D.S., Cairns, N.J., Xie, X., Blazey, T.M., Holtzman, D.M., Santacruz, A., Buckles, V., Oliver, A., Moulder, K., Aisen, P.S., Ghetti, B., Klunk, W.E., McDade, E., Martins, R.N., Masters, C.L., Mayeux, R., Ringman, J.M., Rossor, M.N., Schofield, P.R., Sperling, R.A., Salloway, S., Morris, J.C., 2012. Clinical and Biomarker Changes in Dominantly Inherited Alzheimer's Disease. New England Journal of Medicine 367(9), 795-804.

Bates, T., Strangward, M., J, K., GP, D., PM, M., JB, C., 1996. Inhibition of N-acetylaspartate production: implications for 1H MRS studies in vivo. 7 8, 1397-1400.

Benilova, I., Karran, E., De Strooper, B., 2012. The toxic Aβ oligomer and Alzheimer's disease: an emperor in need of clothes. Nature Neuroscience 15, 349.

Bitsch, A., Bruhn, H., Vougioukas, V., Stringaris, A., Lassmann, H., Frahm, J., Brück, W., 1999. Inflammatory CNS Demyelination: Histopathologic Correlation with In Vivo Quantitative Proton MR Spectroscopy. American Journal of Neuroradiology 20, 1619–1627.

Blatter, D.D., Bigler, E.D., Gale, S.D., Johnson, S.C., Anderson, C.V., Burnett, B.M., Parker, N., Kurth, S., Horn, S.D., 1995. Quantitative volumetric analysis of brain MR: normative database spanning 5 decades of life. American Journal of Neuroradiology 16(2), 241-251.

Blennow, K., Dubois, B., Fagan, A.M., Lewczuk, P., de Leon, M.J., Hampel, H., 2015. Clinical utility of cerebrospinal fluid biomarkers in the diagnosis of early Alzheimer's disease. Alzheimer's & dementia : the journal of the Alzheimer's Association 11(1), 58-69.

Blennow, K., Hampel, H., 2003. CSF markers for incipient Alzheimer's disease. Lancet Neurol 2, 605 - 613.

Blom, E.S., Giedraitis, V., Zetterberg, H., Fukumoto, H., Blennow, K., Hyman, B.T., Irizarry, M.C., Wahlund, L.O., Lannfelt, L., Ingelsson, M., 2009. Rapid Progression from Mild Cognitive Impairment to Alzheimer's Disease in Subjects with Elevated Levels of Tau in Cerebrospinal Fluid and the APOE ε4/ε4 Genotype. Dementia and Geriatric Cognitive Disorders 27(5), 458-464.

Braak, H., Alafuzoff, I., Arzberger, T., Kretzschmar, H., Del Tredici, K., 2006. Staging of Alzheimer disease-associated neurofibrillary pathology using paraffin sections and immunocytochemistry. Acta Neuropathologica 112(4), 389-404.

Braak, H., Braak, E., 1991. Neuropathological stageing of Alzheimer-related changes. Acta Neuropathologica 82(4), 239-259.

Brettschneider, J., Tredici, K.D., Lee, V.M.Y., Trojanowski, J.Q., 2015. Spreading of pathology in neurodegenerative diseases: a focus on human studies. Nature Reviews Neuroscience 16, 109.

Buchhave, P., Minthon, L., Zetterberg, H., Wallin, A., Blennow, K., Hansson, O., 2012. Cerebrospinal fluid levels of beta-amyloid 1-42, but not of tau, are fully changed already 5 to 10 years before the onset of Alzheimer dementia. Arch Gen Psychiatry 69, 98 - 106.

Buckner, R.L., Head, D., Parker, J., Fotenos, A.F., Marcus, D., Morris, J.C., Snyder, A.Z., 2004. A unified approach for morphometric and functional data analysis in young, old, and demented adults using automated atlas-based head size normalization: reliability and validation against manual measurement of total intracranial volume. NeuroImage 23(2), 724-738.

Buckner, R.L., Snyder, A.Z., Shannon, B.J., LaRossa, G., Sachs, R., Fotenos, A.F., Sheline, Y.I., Klunk, W.E., Mathis, C.A., Morris, J.C., Mintun, M.A., 2005. Molecular, structural, and functional characterization of Alzheimer's disease: evidence for a relationship between default activity, amyloid, and memory. J Neurosci 25(34), 7709-7717.

Buñuel, L., 1983. My Last Sigh: The Autobiography of Luis Buñuel. New York: Alfred A. Knopf.

Chételat, G., Villemagne, V.L., Pike, K.E., Ellis, K.A., Bourgeat, P., Jones, G., O'Keefe, G.J., Salvado, O., Szoeke, C., Martins, R.N., Ames, D., Masters, C.L., Rowe, C.C., 2011. Independent contribution of temporal β-amyloid deposition to memory decline in the pre-dementia phase of Alzheimer's disease. Brain 134(3), 798-807.

Coffey, C., Lucke, J.F., Saxton, J.A., et al., 1998. Sex differences in brain aging: A quantitative magnetic resonance imaging study. Archives of Neurology 55(2), 169-179.

Corder, E.H., Saunders, A.M., Strittmatter, W.J., Schmechel, D.E., Gaskell, P.C., Small, G.W., Roses, A.D., Haines, J.L., Pericak-Vance, M.A., 1993. Gene dose of apolipoprotein E type 4 allele and the risk of Alzheimer's disease in late onset families. Science 261(5123), 921-923.

Courchesne, E., Chisum, H.J., Townsend, J., Cowles, A., Covington, J., Egaas, B., Harwood, M., Hinds, S., Press, G.A., 2000. Normal Brain Development and Aging: Quantitative Analysis at in Vivo MR Imaging in Healthy Volunteers. Radiology 216(3), 672-682.

Dai, G., Yu, H., Kruse, M., Traynor-Kaplan, A., Hille, B., 2016. Osmoregulatory inositol transporter SMIT1 modulates electrical activity by adjusting PI(4,5)P2 levels. Proceedings of the National Academy of Sciences 113(23), E3290-E3299.

Dai, Z., He, Y., 2014. Disrupted structural and functional brain connectomes in mild cognitive impairment and Alzheimer’s disease. Neuroscience Bulletin 30(2), 217-232.

Dautry, C., Françoise, V., Emmanuel, B., Nicolas, B., Pierre-Gilles, H., Françoise, C., Gilles, B., Philippe, H., 2000. Early N-Acetylaspartate Depletion Is a Marker of Neuronal Dysfunction in Rats and Primates Chronically Treated with the Mitochondrial Toxin 3-Nitropropionic Acid. Journal of Cerebral Blood Flow & Metabolism 20(5), 789-799.

Deary, I.J., Corley, J., Gow, A.J., Harris, S.E., Houlihan, L.M., Marioni, R.E., Penke, L., Rafnsson, S.B., Starr, J.M., 2009. Age-associated cognitive decline. British Medical Bulletin 92(1), 135-152.

deBruijn, R.F.A.G., Bos, M.J., Portegies, M.L.P., Hofman, A., Franco, O.H., Koudstaal, P.J., Ikram, M.A., 2015. The potential for prevention of dementia across two decades: the prospective, population-based Rotterdam Study. BMC Medicine 13(1), 132.

Desikan, R.S., Ségonne, F., Fischl, B., Quinn, B.T., Dickerson, B.C., Blacker, D., Buckner, R.L., Dale, A.M., Maguire, R.P., Hyman, B.T., Albert, M.S., Killiany, R.J., 2006. An automated labeling system for subdividing the human cerebral cortex on MRI scans into gyral based regions of interest. NeuroImage 31(3), 968-980.

Dickerson, B.C., Bakkour, A., Salat, D.H., Feczko, E., Pacheco, J., Greve, D.N., Grodstein, F., Wright, C.I., Blacker, D., Rosas, H.D., Sperling, R.A., Atri, A., Growdon, J.H., Hyman, B.T., Morris, J.C., Fischl, B., Buckner, R.L., 2009. The Cortical Signature of Alzheimer's Disease: Regionally Specific Cortical Thinning Relates to Symptom Severity in Very Mild to Mild AD Dementia and is Detectable in Asymptomatic Amyloid-Positive Individuals. Cerebral Cortex (New York, NY) 19(3), 497-510.

Dickerson, B.C., Wolk, D.A., 2012. MRI cortical thickness biomarker predicts AD-like CSF and cognitive decline in normal adults. Neurology 78(2), 84-90.

Dubois, B., Feldman, H.H., Jacova, C., Hampel, H., Molinuevo, J.L., Blennow, K., DeKosky, S.T., Gauthier, S., Selkoe, D., Bateman, R., Cappa, S., Crutch, S., Engelborghs, S., Frisoni, G.B., Fox, N.C., Galasko, D., Habert, M.-O., Jicha, G.A., Nordberg, A., Pasquier, F., Rabinovici, G., Robert, P., Rowe, C., Salloway, S., Sarazin, M., Epelbaum, S., de Souza, L.C., Vellas, B., Visser, P.J., Schneider, L., Stern, Y., Scheltens, P., Cummings, J.L., 2014. Advancing research diagnostic criteria for Alzheimer's disease: the IWG-2 criteria. The Lancet Neurology 13(6), 614-629.

Fagan, A.M., Roe, C.M., Xiong, C., Mintun, M.A., Morris, J.C., Holtzman, D.M., 2007. Cerebrospinal fluid tau/β-amyloid42 ratio as a prediction of cognitive decline in nondemented older adults. Archives of Neurology 64(3), 343-349.

Farrell, M.E., Kennedy, K.M., Rodrigue, K.M., et al., 2017. Association of longitudinal cognitive decline with amyloid burden in middle-aged and older adults: Evidence for a dose-response relationship. JAMA Neurology 74(7), 830-838.

Farrer, L.A., Cupples, L., Haines, J.L., et al., 1997. Effects of age, sex, and ethnicity on the association between apolipoprotein e genotype and alzheimer disease: A meta-analysis. JAMA 278(16), 1349-1356.

Ferreira, D., Verhagen, C., Hernández-Cabrera, J.A., Cavallin, L., Guo, C.-J., Ekman, U., Muehlboeck, J.S., Simmons, A., Barroso, J., Wahlund, L.-O., Westman, E., 2017. Distinct subtypes of Alzheimer's disease based on patterns of brain atrophy: longitudinal trajectories and clinical applications. Scientific Reports 7, 46263.

Fischl, B., Dale, A.M., 2000. Measuring the thickness of the human cerebral cortex from magnetic resonance images. Proc Natl Acad Sci U S A 97(20), 11050-11055.

Fischl, B., Salat, D.H., Busa, E., Albert, M., Dieterich, M., Haselgrove, C., van der Kouwe, A., Killiany, R., Kennedy, D., Klaveness, S., Montillo, A., Makris, N., Rosen, B., Dale, A.M., 2002. Whole brain segmentation: automated labeling of neuroanatomical structures in the human brain. Neuron 33(3), 341-355.

Fischl, B., Sereno, M.I., Dale, A.M., 1999. Cortical surface-based analysis. II: Inflation, flattening, and a surface-based coordinate system. Neuroimage 9(2), 195-207.

Fischl, B., van der Kouwe, A., Destrieux, C., Halgren, E., Segonne, F., Salat, D.H., Busa, E., Seidman, L.J., Goldstein, J., Kennedy, D., Caviness, V., Makris, N., Rosen, B., Dale, A.M., 2004. Automatically parcellating the human cerebral cortex. Cereb Cortex 14(1), 11-22.

Fisher, S., Novak, J., Agranoff, B., 2002. Inositol and higher inositol phosphates in neural tissues: homeostasis, metabolism and functional significance. Journal of Neurochemistry 82(4), 736-754.

Fjell, A.M., McEvoy, L., Holland, D., Dale, A.M., Walhovd, K.B., 2014. What is normal in normal aging? Effects of aging, amyloid and Alzheimer's disease on the cerebral cortex and the hippocampus. Progress in Neurobiology 117, 20-40.

Fjell, A.M., Walhovd, K.B., Fennema-Notestine, C., McEvoy, L.K., Hagler, D.J., Holland, D., Brewer, J.B., Dale, A.M., 2009. One year brain atrophy evident in healthy aging. The Journal of neuroscience : the official journal of the Society for Neuroscience 29(48), 15223-15231.

Fox, N.C., Cousens, S., Scahill, R., Harvey, R.J., Rossor, M.N., 2000. Using serial registered brain magnetic resonance imaging to measure disease progression in alzheimer disease: Power calculations and estimates of sample size to detect treatment effects. Archives of Neurology 57(3), 339-344.

Fox, N.C., Warrington, E.K., Freeborough, P.A., Hartikainen, P., Kennedy, A.M., Stevens, J.M., Rossor, M.N., 1996. Presymptomatic hippocampal atrophy in Alzheimer's disease. A longitudinal MRI study. Brain 119 (Pt 6), 2001-2007.

Frisoni, G.B., Fox, N.C., Jack, C.R., Scheltens, P., Thompson, P.M., 2010. The clinical use of structural MRI in Alzheimer disease. Nat Rev Neurol 6(2), 67-77.

Giannakopoulos, P., Herrmann, F.R., Bussière, T., Bouras, C., Kövari, E., Perl, D.P., Morrison, J.H., Gold, G., Hof, P.R., 2003. Tangle and neuron numbers, but not amyloid load, predict cognitive status in Alzheimer's disease. pp. 1495-1500.

Glenner, G.G., Wong, C.W., 1984. Alzheimer's disease: initial report of the purification and characterization of a novel cerebrovascular amyloid protein. Biochem Biophys Res Commun 120(3), 885-890.

Godbolt, A.K., Waldman, A.D., MacManus, D.G., Schott, J.M., Frost, C., Cipolotti, L., Fox, N.C., Rossor, M.N., 2006. MRS shows abnormalities before symptoms in familial Alzheimer disease. Neurology 66(5), 718-722.

Gold, C.A., Budson, A.E., 2008. Memory loss in Alzheimer's disease: implications for development of therapeutics. Expert review of neurotherapeutics 8(12), 1879-1891.

Gomar, J.J., Gordon, M.L., Dickinson, D., Kingsley, P.B., Uluğ, A.M., Keehlisen, L., Huet, S., Buthorn, J.J., Koppel, J., Christen, E., Conejero-Goldberg, C., Davies, P., Goldberg, T.E., 2013. APOE Genotype Modulates Proton Magnetic Resonance Spectroscopy Metabolites in the Aging Brain. Biological Psychiatry 75(9), 686-692.

Good, C.D., Johnsrude, I.S., Ashburner, J., Henson, R.N.A., Friston, K.J., Frackowiak, R.S.J., 2001. A Voxel-Based Morphometric Study of Ageing in 465 Normal Adult Human Brains. NeuroImage 14(1), 21-36.

Graves, A.B., Mortimer, J.A., Larson, E.B., Wenzlow, A., Bowen, J.D., McCormick, W.C., 1996. Head Circumference as a Measure of Cognitive Reserve: Association with Severity of Impairment in Alzheimer's Disease. British Journal of Psychiatry 169(1), 86-92.

Greicius, M.D., Supekar, K., Menon, V., Dougherty, R.F., 2009. Resting-State Functional Connectivity Reflects Structural Connectivity in the Default Mode Network. Cerebral Cortex 19(1), 72-78.

Grundke-Iqbal, I., Iqbal, K., Tung, Y.C., Quinlan, M., Wisniewski, H.M., Binder, L.I., 1986. Abnormal phosphorylation of the microtubule-associated protein tau (tau) in Alzheimer cytoskeletal pathology. Proceedings of the National Academy of Sciences 83(13), 4913.

Gur, R.C., Mozley, P.D., Resnick, S.M., Gottlieb, G.L., Kohn, M., Zimmerman, R., Herman, G., Atlas, S., Grossman, R., Berretta, D., 1991. Gender differences in age effect on brain atrophy measured by magnetic resonance imaging. PNAS 88(7), 2845-2849.

Gómez-Isla, T., Hollister, R., West, H., Mui, S., Growdon, J.H., Petersen, R.C., Parisi, J.E., Hyman, B.T., 1997. Neuronal loss correlates with but exceeds neurofibrillary tangles in Alzheimer's disease. Annals of Neurology 41(1), 17-24.

Haass, C., Selkoe, D.J., 2007. Soluble protein oligomers in neurodegeneration: lessons from the Alzheimer's amyloid β-peptide. Nature Reviews Molecular Cell Biology 8, 101.

Hampel, H., Frank, R., Broich, K., Teipel, S.J., Katz, R.G., Hardy, J., Herholz, K., Bokde, A.L.W., Jessen, F., Hoessler, Y.C., Sanhai, W.R., Zetterberg, H., Woodcock, J., Blennow, K., 2010. Biomarkers for Alzheimer's disease: academic, industry and regulatory perspectives. Nature Reviews Drug Discovery 9, 560.

Hampel, H., O'Bryant, S.E., Castrillo, J.I., Ritchie, C., Rojkova, K., Broich, K., Benda, N., Nisticò, R., Frank, R.A., Dubois, B., Escott-Price, V., Lista, S., 2016. PRECISION MEDICINE - The Golden Gate for Detection, Treatment and Prevention of Alzheimer's Disease. The journal of prevention of Alzheimer's disease 3(4), 243-259.

Harada, C.N., Natelson Love, M.C., Triebel, K., 2013. Normal Cognitive Aging. Clinics in geriatric medicine 29(4), 737-752.

He, Y., Chen, Z., Evans, A., 2008. Structural Insights into Aberrant Topological Patterns of Large-Scale Cortical Networks in Alzheimer's Disease. The Journal of Neuroscience 28(18), 4756-4766.

Hill, N.L., Mogle, J., Wion, R., Munoz, E., DePasquale, N., Yevchak, A.M., Parisi, J.M., 2016. Subjective Cognitive Impairment and Affective Symptoms: A Systematic Review. The Gerontologist 56(6), e109-e127.

Holmes, C., Boche, D., Wilkinson, D., Yadegarfar, G., Hopkins, V., Bayer, A., Jones, R.W., Bullock, R., Love, S., Neal, J.W., Zotova, E., Nicoll, J.A.R., 2008. Long-term effects of Aβ42 immunisation in Alzheimer's disease: follow-up of a randomised, placebo-controlled phase I trial. The Lancet 372(9634), 216-223.

Huang, W., Alexander, G.E., Chang, L., Shetty, H.U., Krasuski, J.S., Rapoport, S.I., Schapiro, M.B., 2001. Brain metabolite concentration and dementia severity in Alzheimer's disease: a (1)H MRS study. Neurology 57(4), 626-632.

Huang, W., Alexander, G.E., Daly, E.M., Shetty, H.U., Krasuski, J.S., Rapoport, S.I., Schapiro, M.B., 1999. High Brain myo-Inositol Levels in the Predementia Phase of Alzheimer's Disease in Adults With Down's Syndrome: A 1H MRS Study. American Journal of Psychiatry 156(12), 1879-1886.

Hyman, B.T., Marzloff, K., Arriagada, P.V., 1993. The Lack of Accumulation of Senile Plaques or Amyloid Burden in Alzheimer's Disease Suggests a Dynamic Balance Between Amyloid Deposition and Resolution. Journal of Neuropathology & Experimental Neurology 52(6), 594-600.

Ikonomovic, M.D., Klunk, W.E., Abrahamson, E.E., Mathis, C.A., Price, J.C., Tsopelas, N.D., Lopresti, B.J., Ziolko, S., Bi, W., Paljug, W.R., Debnath, M.L., Hope, C.E., Isanski, B.A., Hamilton, R.L., DeKosky, S.T., 2008. Post-mortem correlates of in vivo PiB-PET amyloid imaging in a typical case of Alzheimer's disease. Brain 131(6), 1630-1645.

Iqbal, K., del C. Alonso, A., Chen, S., Chohan, M.O., El-Akkad, E., Gong, C.-X., Khatoon, S., Li, B., Liu, F., Rahman, A., Tanimukai, H., Grundke-Iqbal, I., 2005. Tau pathology in Alzheimer disease and other tauopathies. Biochimica et Biophysica Acta (BBA) - Molecular Basis of Disease 1739(2), 198-210.

Jack, C.R., Bennett, D.A., Blennow, K., Carrillo, M.C., Feldman, H.H., Frisoni, G.B., Hampel, H., Jagust, W.J., Johnson, K.A., Knopman, D.S., Petersen, R.C., Scheltens, P., Sperling, R.A., Dubois, B., 2016. A/T/N: An unbiased descriptive classification scheme for Alzheimer disease biomarkers. Neurology 87(5), 539-547.

Jack, C.R., Jr., Albert, M.S., Knopman, D.S., McKhann, G.M., Sperling, R.A., Carrillo, M.C., Thies, B., Phelps, C.H., 2011. Introduction to the recommendations from the National Institute on Aging-Alzheimer's Association workgroups on diagnostic guidelines for Alzheimer's disease. Alzheimers Dement 7(3), 257-262.

Jack, C.R., Petersen, R.C., Xu, Y.C., O'Brien, P.C., Smith, G.E., Ivnik, R.J., Boeve, B.F., Waring, S.C., Tangalos, E.G., Kokmen, E., 1999. Prediction of AD with MRI-Based Hippocampal Volume in Mild Cognitive Impairment. Neurology 52(7), 1397-1403.

Janelidze, S., Zetterberg, H., Mattsson, N., Palmqvist, S., Vanderstichele, H., Lindberg, O., van Westen, D., Stomrud, E., Minthon, L., Blennow, K., the Swedish Bio, F.s.g., Hansson,

O., 2016. CSF Aβ42/Aβ40 and Aβ42/Aβ38 ratios: better diagnostic markers of Alzheimer disease. Annals of Clinical and Translational Neurology 3(3), 154-165.

Jansen, W.J., Ossenkoppele, R., Knol, D.L., et al., 2015. Prevalence of cerebral amyloid pathology in persons without dementia: A meta-analysis. JAMA 313(19), 1924-1938.

Jenkins, R., Fox, N.C., Rossor, A.M., Harvey, R.J., Rossor, M.N., 2000. Intracranial volume and alzheimer disease: Evidence against the cerebral reserve hypothesis. Archives of Neurology 57(2), 220-224.

Jessen, F., Amariglio, R.E., van Boxtel, M., Breteler, M., Ceccaldi, M., Chételat, G., Dubois, B., Dufouil, C., Ellis, K.A., van der Flier, W.M., Glodzik, L., van Harten, A.C., de Leon, M.J., McHugh, P., Mielke, M.M., Molinuevo, J.L., Mosconi, L., Osorio, R.S., Perrotin, A., Petersen, R.C., Rabin, L.A., Rami, L., Reisberg, B., Rentz, D.M., Sachdev, P.S., de la Sayette, V., Saykin, A.J., Scheltens, P., Shulman, M.B., Slavin, M.J., Sperling, R.A., Stewart, R., Uspenskaya, O., Vellas, B., Visser, P.J., Wagner, M., 2014. A conceptual framework for research on subjective cognitive decline in preclinical Alzheimer's disease. Alzheimer's & Dementia 10(6), 844-852.

Jessen, F., Lewczuk, P., Gür, O., Block, W., Ende, G., Frölich, L., Hammen, T., Arlt, S., Kornhuber, J., Kucinski, T., Popp, J., Peters, O., Maier, W., Träber, F., Wiltfang, J., 2011. Association of N-Acetylaspartate and Cerebrospinal Fluid Aβ42 in Dementia. Journal of Alzheimer's Disease 27(2), 393-399.

Kanekiyo, T., Xu, H., Bu, G., 2014. ApoE and Aβ in Alzheimer's Disease: Accidental Encounters or Partners? Neuron 81(4), 740-754.

Kantarci, K., 2013. Proton MRS in mild cognitive impairment. Journal of Magnetic Resonance Imaging 37(4), 770-777.

Kantarci, K., Weigand, S.D., Przybelski, S.A., Preboske, G.M., Pankratz, V.S., Vemuri, P., Senjem, M.L., Murphy, M.C., Gunter, J.L., Machulda, M.M., Ivnik, R.J., Roberts, R.O., Boeve, B.F., Rocca, W.A., Knopman, D.S., Petersen, R.C., Jack, C.R., 2013. MRI and MRS predictors of mild cognitive impairment in a population-based sample. Neurology 81(2), 126-133.

Kantarci, K., Xu, Y., Shiung, M.M., O'Brien, P.C., Cha, R.H., Smith, G.E., Ivnik, R.J., Boeve, B.F., Edland, S.D., Kokmen, E., Tangalos, E.G., Petersen, R.C., Jack Jr, C.R., 2002. Comparative Diagnostic Utility of Different MR Modalities in Mild Cognitive Impairment and Alzheimer's Disease. Dementia and Geriatric Cognitive Disorders 14(4), 198-207.

Kivipelto, M., Ngandu, T., Fratiglioni, L., et al., 2005. Obesity and vascular risk factors at midlife and the risk of dementia and alzheimer disease. Archives of Neurology 62(10), 1556-1560.

Klein, J., 2000. Membrane breakdown in acute and chronic neurodegeneration: focus on choline-containing phospholipids. Journal of Neural Transmission 107(8), 1027-1063.

Kwon, H.M., Yamauchi, A., Uchida, S., Preston, A.S., Garcia-Perez, A., Burg, M.B., Handler, J.S., 1992. Cloning of the cDNa for a Na+/myo-inositol cotransporter, a hypertonicity stress protein. Journal of Biological Chemistry 267(9), 6297-6301.

Latora, V., Marchiori, M., 2001. Efficient Behavior of Small-World Networks. Physical Review Letters 87(19), 198701.

Lee, J.H., Arcinue, E., Ross, B.D., 1994. Organic Osmolytes in the Brain of an Infant with Hypernatremia. New England Journal of Medicine 331(7), 439-442.

Lehmann, M., Rohrer, J.D., Clarkson, M.J., Ridgway, G.R., Scahill, R.I., Modat, M., Warren, J.D., Ourselin, S., Barnes, J., Rossor, M.N., Fox, N.C., 2010. Reduced Cortical Thickness in the Posterior Cingulate Gyrus is Characteristic of Both Typical and Atypical Alzheimer's Disease. Journal of Alzheimer's Disease 20(2), 587-598.

Lind, L., Fors, N., Hall, J., Marttala, K., Stenborg, A., 2006. A comparison of three different methods to determine artierial compliance in the elderly: the Prospective Investigation of the Vasculature in Uppsala Seniors (PIVUS) study. J Hypertens. 24(6), 1075-1082.

Litjens, G., Kooi, T., Bejnordi, B.E., Setio, A.A.A., Ciompi, F., Ghafoorian, M., van der Laak, J.A.W.M., van Ginneken, B., Sánchez, C.I., 2017. A survey on deep learning in medical image analysis. Medical Image Analysis 42, 60-88.

Liu, C.-C., Kanekiyo, T., Xu, H., Bu, G., 2013. Apolipoprotein E and Alzheimer disease: risk, mechanisms and therapy. Nat Rev Neurol 9(2), 106-118.

Lynn, M.B., Chang-En, Y., Thomas, D.B., Debby, W.T., 2010. Review Article: Genetics of Alzheimer Disease. Journal of Geriatric Psychiatry and Neurology 23(4), 213-227.

Maddock, R., Buonocore, M., 2012. MR Spectroscopic Studies of the Brain in Psychiatric Disorders, in: Carter, C.S., Dalley, J.W. (Eds.), Brain Imaging in Behavioral Neuroscience. Springer Berlin Heidelberg, pp. 199-251.

Mariani, E., Monastero, R., Mecocci, P., 2007. Mild Cognitive Impairment: A Systematic Review Journal of Alzheimer's Disease, pp. 23-35.

Marjańska, M., Weigand, S.D., Preboske, G., Wengenack, T.M., Chamberlain, R., Curran, G.L., Poduslo, J.F., Garwood, M., Kobayashi, D., Lin, J.C., Jack, C.R., 2014. Treatment Effects in a Transgenic Mouse Model of Alzheimer’s Disease: A Magnetic Resonance Spectroscopy Study after Passive Immunization. Neuroscience 259, 94-100.

Martínez-Bisbal, M.C., Arana, E., Martí-Bonmatí, L., Mollá, E., Celda, B., 2004. Cognitive impairment: classification by 1H magnetic resonance spectroscopy. European Journal of Neurology 11(3), 187-193.

Masters, C.L., Simms, G., Weinman, N.A., Multhaup, G., McDonald, B.L., Beyreuther, K., 1985. Amyloid plaque core protein in Alzheimer disease and Down syndrome. Proc Natl Acad Sci U S A 82(12), 4245-4249.

Mattsson, N., Insel, P.S., Aisen, P.S., Jagust, W., Mackin, S., Weiner, M., 2015. Brain structure and function as mediators of the effects of amyloid on memory. Neurology 84(11), 1136.

Maurer, K., Volk, S., Gerbaldo, H., 1997. Auguste D and Alzheimer's disease. The Lancet 349(9064), 1546-1549.

McKhann, G., Drachman, D., Folstein, M., Katzman, R., Price, D., Stadlan, E.M., 1984. Clinical diagnosis of Alzheimer's disease: report of the NINCDS-ADRDA Work Group under the auspices of Department of Health and Human Services Task Force on Alzheimer's Disease. Neurology 34(7), 939-944.

McKhann, G.M., Knopman, D.S., Chertkow, H., Hyman, B.T., Jack, C.R., Jr., Kawas, C.H., Klunk, W.E., Koroshetz, W.J., Manly, J.J., Mayeux, R., Mohs, R.C., Morris, J.C., Rossor, M.N., Scheltens, P., Carrillo, M.C., Thies, B., Weintraub, S., Phelps, C.H., 2011. The diagnosis of dementia due to Alzheimer's disease: Recommendations from the National Institute on Aging-Alzheimer's Association workgroups on diagnostic guidelines for Alzheimer's disease. Alzheimers Dement 7(3), 263-269.

Mijalkov, M., Kakaei, E., Pereira, J.B., Westman, E., Volpe, G., 2017. BRAPH: A Graph Theory Software for the Analysis of Brain Connectivity. bioRxiv 106625.

Minoshima, S., Giordani, B., Berent, S., Frey, K., Foster, N., Kuhl, D., 1997. Metabolic reduction in the posterior cingulate cortex in very early Alzheimer's disease. Ann Neurol. 42(1), 85-94.

Mitchell, A.J., Beaumont, H., Ferguson, D., Yadegarfar, M., Stubbs, B., 2014. Risk of dementia and mild cognitive impairment in older people with subjective memory complaints: meta-analysis. Acta Psychiatrica Scandinavica 130(6), 439-451.

Mlynárik, V., Cudalbu, C., Xin, L., Gruetter, R., 2008. 1H NMR spectroscopy of rat brain in vivo at 14.1Tesla: Improvements in quantification of the neurochemical profile. Journal of Magnetic Resonance 194(2), 163-168.

Moffett, J.R., Ross, B., Arun, P., Madhavarao, C.N., Namboodiri, A.M.A., 2007. N-Acetylaspartate in the CNS: From neurodiagnostics to neurobiology. Progress in Neurobiology 81(2), 89-131.

Mormino, E.C., Smiljic, A., Hayenga, A.O., H. Onami, S., Greicius, M.D., Rabinovici, G.D., Janabi, M., Baker, S.L., V. Yen, I., Madison, C.M., Miller, B.L., Jagust, W.J., 2011. Relationships between Beta-Amyloid and Functional Connectivity in Different Components of the Default Mode Network in Aging. Cerebral Cortex 21(10), 2399-2407.

Morris, M., Maeda, S., Vossel, K., Mucke, L., 2011. The Many Faces of Tau. Neuron 70(3), 410-426.

Mosconi, L., 2013. Glucose metabolism in normal aging and Alzheimer’s disease: Methodological and physiological considerations for PET studies. Clinical and translational imaging : reviews in nuclear medicine and molecular imaging 1(4), 10.1007/s40336-40013-40026-y.

Murray, M.E., Graff-Radford, N.R., Ross, O.A., Petersen, R.C., Duara, R., Dickson, D.W., 2011. Neuropathologically defined subtypes of Alzheimer's disease with distinct clinical characteristics: A retrospective study. Lancet neurology 10(9), 785-796.

Murray, M.E., Przybelski, S.A., Lesnick, T.G., Liesinger, A.M., Spychalla, A., Zhang, B., Gunter, J.L., Parisi, J.E., Boeve, B.F., Knopman, D.S., Petersen, R.C., Jack, C.R., Dickson, D.W., Kantarci, K., 2014. Early Alzheimer's Disease Neuropathology Detected by Proton MR Spectroscopy. The Journal of Neuroscience 34(49), 16247-16255.

Murray, M.E., Przybelski, S.A., Lesnick, T.G., Liesinger, A.M., Spychalla, A., Zhang, B., Gunter, J.L., Parisi, J.E., Boeve, B.F., Knopman, D.S., Petersen, R.C., Jack, C.R., Jr., Dickson, D.W., Kantarci, K., 2014. Early Alzheimer's disease neuropathology detected by proton MR spectroscopy. J Neurosci 34(49), 16247-16255.

Nedelska, Z., Przybelski, S.A., Lesnick, T.G., Schwarz, C.G., Lowe, V.J., Machulda, M.M., Kremers, W.K., Mielke, M.M., Roberts, R.O., Boeve, B.F., Knopman, D.S., Petersen, R.C., Jack, C.R., Kantarci, K., 2017. 1H-MRS metabolites and rate of β-amyloid accumulation on serial PET in clinically normal adults. Neurology.

Newman, M.E.J., 2003. The Structure and Function of Complex Networks. SIAM Review 45(2), 167-256.

Newman, M.E.J., 2006. Modularity and community structure in networks. Proceedings of the National Academy of Sciences 103(23), 8577-8582.

Ngandu, T., Lehtisalo, J., Solomon, A., Levälahti, E., Ahtiluoto, S., Antikainen, R., Bäckman, L., Hänninen, T., Jula, A., Laatikainen, T., Lindström, J., Mangialasche, F., Paajanen, T., Pajala, S., Peltonen, M., Rauramaa, R., Stigsdotter-Neely, A., Strandberg, T., Tuomilehto, J., Soininen, H., Kivipelto, M., 2015. A 2 year multidomain intervention of diet, exercise, cognitive training, and vascular risk monitoring versus control to prevent cognitive decline in at-risk elderly people (FINGER): a randomised controlled trial. The Lancet 385(9984), 2255-2263.

Nordenskjöld, R., Malmberg, F., Larsson, E.-M., Simmons, A., Brooks, S.J., Lind, L., Ahlström, H., Johansson, L., Kullberg, J., 2013. Intracranial volume estimated with commonly used methods could introduce bias in studies including brain volume measurements. NeuroImage 83(0), 355-360.

Olsson, B., Lautner, R., Andreasson, U., Öhrfelt, A., Portelius, E., Bjerke, M., Hölttä, M., Rosén, C., Olsson, C., Strobel, G., Wu, E., Dakin, K., Petzold, M., Blennow, K., Zetterberg, H., 2016. CSF and blood biomarkers for the diagnosis of Alzheimer's disease: a systematic review and meta-analysis. The Lancet Neurology 15(7), 673-684.

Ossenkoppele, R., Schonhaut, D.R., Schöll, M., Lockhart, S.N., Ayakta, N., Baker, S.L., O'Neil, J.P., Janabi, M., Lazaris, A., Cantwell, A., Vogel, J., Santos, M., Miller, Z.A., Bettcher, B.M., Vossel, K.A., Kramer, J.H., Gorno-Tempini, M.L., Miller, B.L., Jagust, W.J., Rabinovici, G.D., 2016. Tau PET patterns mirror clinical and neuroanatomical variability in Alzheimer's disease. Brain 139(5), 1551-1567.

Pacheco, J., Goh, J.O., Kraut, M.A., Ferrucci, L., Resnick, S.M., 2015. Greater cortical thinning in normal older adults predicts later cognitive impairment. Neurobiology of Aging 36(2), 903-908.

Palmqvist, S., Schöll, M., Strandberg, O., Mattsson, N., Stomrud, E., Zetterberg, H., Blennow, K., Landau, S., Jagust, W., Hansson, O., 2017. Earliest accumulation of β-amyloid occurs within the default-mode network and concurrently affects brain connectivity. Nature Communications 8(1), 1214.

Pereira, J.B., Aarsland, D., Ginestet, C.E., Lebedev, A.V., Wahlund, L.-O., Simmons, A., Volpe, G., Westman, E., 2015. Aberrant cerebral network topology and mild cognitive impairment in early Parkinson's disease. Human Brain Mapping 36(8), 2980-2995.

Petersen, R.C., 2004. Mild cognitive impairment as a diagnostic entity. Journal of Internal Medicine 256(3), 183-194.

Petersen, R.C., Parisi, J.E., Dickson, D.W., et al., 2006. Neuropathologic features of amnestic mild cognitive impairment. Archives of Neurology 63(5), 665-672.

Petersen, R.C., Roberts, R.O., Knopman, D.S., Geda, Y.E., Cha, R.H., Pankratz, V.S., Boeve, B.F., Tangalos, E.G., Ivnik, R.J., Rocca, W.A., 2010. Prevalence of mild cognitive impairment is higher in men. Neurology 75(10), 889.

Petersen, R.C., Smith, G.E., Waring, S.C., Ivnik, R.J., Tangalos, E.G., Kokmen, E., 1999. Mild Cognitive Impairment: Clinical Characterization and Outcome. Arch Neurol 56(3), 303-308.

Poulakis, K., Pereira, J.B., Mecocci, P., Vellas, B., Tsolaki, M., Kłoszewska, I., Soininen, H., Lovestone, S., Simmons, A., Wahlund, L.-O., Westman, E., 2018. Heterogeneous patterns of brain atrophy in Alzheimer's disease. Neurobiology of Aging 65, 98-108.

Provencher, S.W., 1993. Estimation of metabolite concentrations from localized in vivo proton NMR spectra. Magn Reson Med 30(6), 672-679.

Provencher, S.W., 2001. Automatic quantitation of localized in vivo 1H spectra with LCModel. NMR Biomed 14(4), 260-264.

Rackayova, V., Cudalbu, C., Pouwels, P.J.W., Braissant, O., 2017. Creatine in the central nervous system: From magnetic resonance spectroscopy to creatine deficiencies. Analytical Biochemistry 529, 144-157.

Raz, N., Gunning-Dixon, F., Head, D., Rodrigue, K.M., Williamson, A., Acker, J.D., 2004. Aging, sexual dimorphism, and hemispheric asymmetry of the cerebral cortex: replicability of regional differences in volume. Neurobiology of Aging 25(3), 377-396.

Reiman, E.M., Chen, K., Liu, X., Bandy, D., Yu, M., Lee, W., Ayutyanont, N., Keppler, J., Reeder, S.A., Langbaum, J.B.S., Alexander, G.E., Klunk, W.E., Mathis, C.A., Price, J.C., Aizenstein, H.J., DeKosky, S.T., Caselli, R.J., 2009. Fibrillar amyloid-β burden in cognitively normal people at 3 levels of genetic risk for Alzheimer's disease. Proceedings of the National Academy of Sciences 106(16), 6820-6825.

Reiman, E.M., Uecker, A., Caselli, R.J., Lewis, S., Bandy, D., De Leon, M.J., De Santi, S., Convit, A., Osborne, D., Weaver, A., Thibodeau, S.N., 1998. Hippocampal volumes in cognitively normal persons at genetic risk for Alzheimer's disease. Annals of Neurology 44(2), 288-291.

Resnick, S.M., Sojkova, J., Zhou, Y., An, Y., Ye, W., Holt, D.P., Dannals, R.F., Mathis, C.A., Klunk, W.E., Ferrucci, L., Kraut, M.A., Wong, D.F., 2010. Longitudinal cognitive decline is associated with fibrillar amyloid-beta measured by [¹¹C]PiB. Neurology 74(10), 807.

Rowe, C.C., Villemagne, V.L., 2011. Brain Amyloid Imaging. Journal of Nuclear Medicine 52(11), 1733-1740.

Rubinov, M., Sporns, O., 2010. Complex network measures of brain connectivity: Uses and interpretations. NeuroImage 52(3), 1059-1069.

Sacks, O., 1985. The Man Who Mistook His Wife For A Hat and other clinical tales. New York: Summit Books.

Salloway, S., Sperling, R., Fox, N.C., Blennow, K., Klunk, W., Raskind, M., Sabbagh, M., Honig, L.S., Porsteinsson, A.P., Ferris, S., Reichert, M., Ketter, N., Nejadnik, B., Guenzler, V., Miloslavsky, M., Wang, D., Lu, Y., Lull, J., Tudor, I.C., Liu, E., Grundman, M., Yuen, E., Black, R., Brashear, H.R., 2014. Two Phase 3 Trials of Bapineuzumab in Mild-to-Moderate Alzheimer's Disease. New England Journal of Medicine 370(4), 322-333.

Samgard, K., Zetterberg, H., Blennow, K., Hansson, O., Minthon, L., Londos, E., 2010. Cerebrospinal fluid total tau as a marker of Alzheimer's disease intensity. Int J Geriatr Psychiatry 25, 403 - 410.

Sanfilipo, M.P., Benedict, R.H.B., Zivadinov, R., Bakshi, R., 2004. Correction for intracranial volume in analysis of whole brain atrophy in multiple sclerosis: the proportion vs. residual method. NeuroImage 22(4), 1732-1743.

Scahill, R.I., Frost, C., Jenkins, R., Whitwell, J.L., Rossor, M.N., Fox, N.C., 2003. A longitudinal study of brain volume changes in normal aging using serial registered magnetic resonance imaging. Archives of Neurology 60(7), 989-994.

Schacter, D.L., Addis, D.R., Hassabis, D., Martin, V.C., Spreng, R.N., Szpunar, K.K., 2012. The Future of Memory: Remembering, Imagining, and the Brain. Neuron 76(4), 10.1016/j.neuron.2012.1011.1001.

Scheltens, P., Leys, D., Barkhof, F., Huglo, D., Weinstein, H.C., Vermersch, P., Kuiper, M., Steinling, M., Wolters, E.C., Valk, J., 1992. Atrophy of medial temporal lobes on MRI in "probable" Alzheimer's disease and normal ageing: diagnostic value and neuropsychological correlates. J Neurol Neurosurg Psychiatry 55(10), 967-972.

Schott, J., Bartlett, J., Fox, N., Barnes, J., 2010. Alzheimer's disease neuroimaging initiative I: increased brain atrophy rates in cognitively normal older adults with low cerebrospinal fluid Abeta1-42. Ann Neurol 68, 825 - 834.

Schott, J.M., Frost, C., MacManus, D.G., Ibrahim, F., Waldman, A.D., Fox, N.C., 2010. Short echo time proton magnetic resonance spectroscopy in Alzheimer's disease: a longitudinal multiple time point study.

Schreiner, S.J., Kirchner, T., Narkhede, A., Wyss, M., Van Bergen, J.M.G., Steininger, S.C., Gietl, A., Leh, S.E., Treyer, V., Buck, A., Pruessmann, K.P., Nitsch, R.M., Hock, C., Henning, A., Brickman, A.M., Unschuld, P.G., 2018. Brain amyloid burden and cerebrovascular disease are synergistically associated with neurometabolism in cognitively unimpaired older adults. Neurobiology of Aging 63, 152-161.

Segonne, F., Dale, A.M., Busa, E., Glessner, M., Salat, D., Hahn, H.K., Fischl, B., 2004. A hybrid approach to the skull stripping problem in MRI. Neuroimage 22(3), 1060-1075.

Segonne, F., Pacheco, J., Fischl, B., 2007. Geometrically accurate topology-correction of cortical surfaces using nonseparating loops. IEEE Trans Med Imaging 26(4), 518-529.

Sheline, Y.I., Raichle, M.E., Snyder, A.Z., Morris, J.C., Head, D., Wang, S., Mintun, M.A., 2010. Amyloid Plaques Disrupt Resting State Default Mode Network Connectivity in Cognitively Normal Elderly. Biological Psychiatry 67(6), 584-587.

Signoretti, S., Marmarou, A., Aygok, G.A., Fatouros, P.P., Portella, G., Bullock, R.M., 2008. Assessment of mitochondrial impairment in traumatic brain injury using high-resolution proton magnetic resonance spectroscopy. Journal of Neurosurgery 108(1), 42-52.

Simmons, A., Westman, E., Muehlboeck, S., Mecocci, P., Vellas, B., Tsolaki, M., Kloszewska, I., Wahlund, L.-O., Soininen, H., Lovestone, S., Evans, A., Spenger, C., 2009. MRI Measures of Alzheimer's Disease and the AddNeuroMed Study. Annals of the New York Academy of Sciences 1180(Biomarkers in Brain Disease), 47-55.

Simmons, A., Westman, E., Muehlboeck, S., Mecocci, P., Vellas, B., Tsolaki, M., Kloszewska, I., Wahlund, L-O., Soininen, H., Lovestone, S., Evans, A., Spenger C. for the AddNeuroMed consortium, 2011. The AddNeuroMed framework for multi-centre MRI assessment of longitudinal changes in Alzheimer’s disease : experience from the first 24 months. Int J Geriatr Psychiatry. 2011 Jan;26(1):75-82.

Sindi, S., Mangialasche, F., Kivipelto, M., 2015. Advances in the prevention of Alzheimer's Disease. F1000Prime Reports 7, 50.

Sled, J.G., Zijdenbos, A.P., Evans, A.C., 1998. A nonparametric method for automatic correction of intensity nonuniformity in MRI data. IEEE Trans Med Imaging 17(1), 87-97.

Sowell, E.R., Peterson, B.S., Kan, E., Woods, R.P., Yoshii, J., Bansal, R., Xu, D., Zhu, H., Thompson, P.M., Toga, A.W., 2007. Sex Differences in Cortical Thickness Mapped in 176 Healthy Individuals between 7 and 87 Years of Age. Cerebral Cortex 17(7), 1550-1560.

Sperling, R.A., Aisen, P.S., Beckett, L.A., Bennett, D.A., Craft, S., Fagan, A.M., Iwatsubo, T., Jack, C.R., Kaye, J., Montine, T.J., Park, D.C., Reiman, E.M., Rowe, C.C., Siemers, E., Stern, Y., Yaffe, K., Carrillo, M.C., Thies, B., Morrison-Bogorad, M., Wagster, M.V., Phelps, C.H., 2011. Toward defining the preclinical stages of Alzheimer’s disease:

Recommendations from the National Institute on Aging-Alzheimer's Association workgroups on diagnostic guidelines for Alzheimer's disease. Alzheimer's & dementia : the journal of the Alzheimer's Association 7(3), 280-292.

Spulber, G., Niskanen, E., MacDonald, S., Smilovici, O., Chen, K., Reiman, E.M., Jauhiainen, A.M., Hallikainen, M., Tervo, S., Wahlund, L.-O., Vanninen, R., Kivipelto, M., Soininen, H., 2010. Whole brain atrophy rate predicts progression from MCI to Alzheimer's disease. Neurobiology of Aging 31(9), 1601-1605.

Stelzmann, R.A., Norman Schnitzlein, H., Reed Murtagh, F., 1995. An english translation of alzheimer's 1907 paper, "über eine eigenartige erkankung der hirnrinde". Clinical Anatomy 8(6), 429-431.

Stern, Y., 2012. Cognitive reserve in ageing and Alzheimer's disease. Lancet neurology 11(11), 1006-1012.

Strimbu, K., Tavel, J.A., 2010. What are Biomarkers? Current opinion in HIV and AIDS 5(6), 463-466.

Tate, D.F., Neeley, E.S., Norton, M.C., Tschanz, J.T., Miller, M.J., Wolfson, L., Hulette, C., Leslie, C., Welsh-Bohmer, K.A., Plassman, B., Bigler, E.D., 2011. Intracranial volume and dementia: some evidence in support of the cerebral reserve hypothesis. Brain Research 1385, 151-162.

Terpstra, M., Cheong, I., Lyu, T., Deelchand, D.K., Emir, U.E., Bednařík, P., Eberly, L.E., Öz, G., 2016. Test-retest reproducibility of neurochemical profiles with short-echo, single voxel MRS at 3T and 7T. Magnetic resonance in medicine 76(4), 1083-1091.

Thompson, P.M., Hayashi, K.M., de Zubicaray, G., Janke, A.L., Rose, S.E., Semple, J., Herman, D., Hong, M.S., Dittmer, S.S., Doddrell, D.M., Toga, A.W., 2003. Dynamics of Gray Matter Loss in Alzheimer's Disease. The Journal of Neuroscience 23(3), 994-1005.

Tijms, B.M., Wink, A.M., de Haan, W., van der Flier, W.M., Stam, C.J., Scheltens, P., Barkhof, F., 2013. Alzheimer's disease: connecting findings from graph theoretical studies of brain networks. Neurobiology of Aging 34(8), 2023-2036.

Valenzuela, M.J., Sachdev, P., 2006. Brain reserve and dementia: a systematic review. Psychological Medicine 36(4), 441-454.

Vemuri, P., Jack, C.R., 2010. Role of structural MRI in Alzheimer's disease. Alzheimer's Research & Therapy 2(4), 23.

Vemuri, P., Lesnick, T.G., Przybelski, S.A., et al., 2014. Association of lifetime intellectual enrichment with cognitive decline in the older population. JAMA Neurology 71(8), 1017-1024.

Videen, J.S., Michaelis, T., Pinto, P., Ross, B.D., 1995. Human cerebral osmolytes during chronic hyponatremia. A proton magnetic resonance spectroscopy study. The Journal of Clinical Investigation 95(2), 788-793.

Villemagne, V.L., Burnham, S., Bourgeat, P., Brown, B., Ellis, K.A., Salvado, O., Szoeke, C., Macaulay, S.L., Martins, R., Maruff, P., Ames, D., Rowe, C.C., Masters, C.L., 2013. Amyloid β deposition, neurodegeneration, and cognitive decline in sporadic Alzheimer's disease: a prospective cohort study. The Lancet Neurology 12(4), 357-367.

Walhovd, K.B., Fjell, A.M., Brewer, J., McEvoy, L.K., Fennema-Notestine, C., Hagler, D.J., Jennings, R.G., Karow, D., Dale, A.M., The Alzheimer's Disease Neuroimaging, I., 2010.

Combining MRI, PET and CSF biomarkers in diagnosis and prognosis of Alzheimer's disease. AJNR. American journal of neuroradiology 31(2), 347.

Watts, D.J., Strogatz, S.H., 1998. Collective dynamics of /`small-world/' networks. Nature 393(6684), 440-442.

Westman, E., Aguilar, C., Muehlboeck, J.S., Simmons, A., 2013. Regional magnetic resonance imaging measures for multivariate analysis in Alzheimer's disease and mild cognitive impairment. Brain Topogr 26(1), 9-23.

Westman, E., Spenger, C., Wahlund, L.-O., Lavebratt, C., 2007. Carbamazepine treatment recovered low N-acetylaspartate+N-acetylaspartylglutamate (tNAA) levels in the megencephaly mouse BALB/cByJ-Kv1.1mceph/mceph. Neurobiology of Disease 26(1), 221-228.

Whitwell, J.L., Josephs, K.A., Murray, M.E., Kantarci, K., Przybelski, S.A., Weigand, S.D., Vemuri, P., Senjem, M.L., Parisi, J.E., Knopman, D.S., Boeve, B.F., Petersen, R.C., Dickson, D.W., Jack, C.R., 2008. MRI correlates of neurofibrillary tangle pathology at autopsy: A voxel-based morphometry study. Neurology 71(10), 743-749.

Wiseman, F.K., Al-Janabi, T., Hardy, J., Karmiloff-Smith, A., Nizetic, D., Tybulewicz, V.L.J., Fisher, E.M.C., Strydom, A., 2015. A genetic cause of Alzheimer disease: mechanistic insights from Down syndrome. Nature reviews. Neuroscience 16(9), 564-574.

Wisniewski, T., Goñi, F., 2015. Immunotherapeutic Approaches for Alzheimer’s Disease. Neuron 85(6), 1162-1176.

Yao, Z., Zhang, Y., Lin, L., Zhou, Y., Xu, C., Jiang, T., the Alzheimer's Disease Neuroimaging, I., 2010. Abnormal Cortical Networks in Mild Cognitive Impairment and Alzheimer's Disease. PLoS Comput Biol 6(11), e1001006.

Öz, G., Alger, J.R., Barker, P.B., Bartha, R., Bizzi, A., Boesch, C., Bolan, P.J., Brindle, K.M., Cudalbu, C., Dinçer, A., Dydak, U., Emir, U.E., Frahm, J., González, R.G., Gruber, S., Gruetter, R., Gupta, R.K., Heerschap, A., Henning, A., Hetherington, H.P., Howe, F.A., Hüppi, P.S., Hurd, R.E., Kantarci, K., Klomp, D.W.J., Kreis, R., Kruiskamp, M.J., Leach, M.O., Lin, A.P., Luijten, P.R., Marjańska, M., Maudsley, A.A., Meyerhoff, D.J., Mountford, C.E., Nelson, S.J., Pamir, M.N., Pan, J.W., Peet, A.C., Poptani, H., Posse, S., Pouwels, P.J.W., Ratai, E.-M., Ross, B.D., Scheenen, T.W.J., Schuster, C., Smith, I.C.P., Soher, B.J., Tkáč, I., Vigneron, D.B., Kauppinen, R.A., Group, F.t.M.C., 2014. Clinical Proton MR Spectroscopy in Central Nervous System Disorders. Radiology 270(3), 658-679.